Application of hydrocarbon and perfluorocarbon oxygen vectors to enhance heterologous production of hyaluronic acid in engineered *Bacillus subtilis*

by

Xiang Ren

A thesis

presented to the University of Waterloo

in fulfillment of the

thesis requirement for the degree of

Master of Applied Science

in

Chemical Engineering

Waterloo, Ontario, Canada, 2017

Author's Declaration

This thesis consists of material all of which I authored or co-authored: see Statement of Contributions included in the thesis. This is a true copy of the thesis, including any required final revisions, as accepted by my examiners.

I understand that my thesis may be made electronically available to the public.

Statement of Contributions

I am the sole author of the Chapter 1, 2 and 4.

Chapter 3 was co-authored with my colleague Adam W. Westbrook in discussion part and reviewed by my supervisor C. Perry Chou.

Abstract

In microbial cultivations for hyaluronic acid (HA) production, oxygen can be a limiting substrate due to its poor solubility in aqueous medium and the substantial increase in culture viscosity at relatively low HA titers. Shear stress due to the high agitation and aeration rates required to overcome oxygen limitation may reduce the quality (i.e. molecular weight) of HA, and production costs associated with power consumption and supplemental oxygen may be excessive. Here, we report the application of oxygen vectors to the heterologous production of HA in engineered *Bacillus subtilis*, leading to significantly improved culture performance. We first derived an improved HA-producing strain of *B. subtilis* through engineering of the promoter driving coexpression of *seHas* and *tuaD*, leading to high-level HA production. Out of seven potential oxygen vectors evaluated in a preliminary screening, significant improvements to the HA titer and/or cell density were observed in cultures containing *n*-heptane, *n*-hexadecane, perfluoromethyldecalin, and perfluoro-1,3-dimethylcyclohexane. Adjustments to the vector concentration, timing of vector addition, and the agitation rate resulted in further enhancements, with the HA titer reaching up to 4.5 g/L after only 10 h cultivation. Moreover, our results indicate that certain vectors may alter the functional expression of Class I hyaluronan synthase (HAS) in *B. subtilis*, and that higher shear rates may drive more carbon flux through the HA biosynthetic pathway without negatively affecting the MW. Our study demonstrates the efficacy of oxygen vectors to enhance heterologous HA production in *B. subtilis*, and provides valuable insight for future bioprocess development in microbial HA production.

Acknowledgements

I wish to begin by acknowledging the guidance and support provided by my supervisors Dr. C. P. Chou and Dr. M. Moo-Young. Your encouragement and scientific expertise were critical for the successful completion of this project and my professional development.

I sincerely thank the Dr. W. Anderson & Dr. D. Simakov for serving on the members of my reading committee and precious advice for my academic thesis. I would also like to thank all colleagues in Dr. C. P. Chou's lab for their insightful technical help and discussions.

Last but certainly not least, I would not be where I am today without the love and support of my family. You all made this possible and never gave up on me, thank you!

Table of Contents

List of Figures

List of Tables

List of Abbreviations

ATP	Nucleoside triphosphate
DNA	Deoxyribonucleic acid
DO	Dissolved oxygen
GlcNAc	*N*-acetyl-D-glucosamine
GlcUA	D-glucuronic acid
HA	Hyaluronic acid
HC	Hydrocarbon
HCD	High cell density
HPLC	High performance liquid chromatography
LB	Lysogeny broth
LED	Light-emitting diode
LHS	Left hand side
MDa	MDalton (the atomic mass unit)
MW	Molecular weight
NADH	The reduced form of Nicotinamide adenine dinucleotide
NAD+	The oxidized form of Nicotinamide adenine dinucleotide
OTR	Oxygen transfer rate
OUR	Oxygen uptake rate
PBS	Phosphate buffered saline
PFC	Perfluorocarbon
STR	Stirred tank reactor

List of Symbols

a	Interfacial area
C^*	Saturation concentration of oxygen in bulk liquid
C_L	Time dependent concentration of oxygen in bulk liquid
D	Diffusivity of oxygen in water
f_V	Volume fraction
k_L	Local liquid-phase mass transfer coefficient
k_La	Volumetric liquid-phase mass transfer coefficient
N	Stirrer speed
N_c	Critical stirrer speed
R	Radii
S	Spreading coefficient
T	Relation time
t	Time
t_e	Exposure time for mass transfer
V_s	Superficial gas velocity
ε	Energy dissipation rate of turbulence
μ_e	Effective dynamic liquid viscosity
v	Kinematic viscosity
ρ	Fluid density
ϕ	Gas holdup
σ	Interfacial tension

Chapter 1- Overview

1.1 Research background

Hyaluronic acid (HA), a linear, unbranched polysaccharide consisting of alternating *N*-acetyl-d-glucosamine and d-glucuronic acid [1], is a valuable biopolymer used in food, cosmetics, pharmaceuticals and the medical field including skin moisturizers, ophthalmic surgery and wound healing [2]. At present, the US market for HA is estimated at over $1 billion annually, and is expected to rapidly increase with the demand for viscosupplements and dermal fillers [3]. Recently, in an effort to avoid the risk of cross-species viral infection, scientists have drawn attention to producing HA from microbials other than from rooster combs traditionally [2]. HA can be synthesized from certain attenuated strains of group C *Streptococcus* naturally as part of their outer capsule [4]. However, due to the challenging and difficulties in expensive fermentation and genetical manipulation in *Streptococci*, it would be advantageous to develop an alternative source of HA, and meanwhile the hasA gene from *Streptococcus equisimilis*, which encodes the enzyme hyaluronan synthase, has been expressed in *Bacillus subtilis*, resulting in the production of HA [2]. As a GRAS (generally recognized as safe) organism, *B. subtilis* is an ideal candidate for production of biopolymers and biofuels [2]. *Bacillus subtilis* is a model Gram-positive organism sought after for its robust growth characteristics in inexpensive media, genetic tractability and ability to secrete products into the extracellular environment. Although *B. subtilis* has gained widespread acceptance as an industrial workhorse for the production of low-cost enzymes or some biopolymers, its status as a recombinant protein expression host has been hindered by issues with protein degradation and misfolding,

and plasmid instability. *B. subtilis* is a heterotrophic organism, which means they need to absorb nutrients from the environment; those nutrients then will be converted into energy in some way. *B. subtilis* can make it without oxygen, so it belongs to the facultative anaerobes. However, based on the previous investigations, the biosynthesis of HA is the oxygen-consuming process which requires abundant oxygen to generate ATPs.

Industrial bioprocesses based on microbial platforms are typically aerobic and are carried out in aqueous growth media containing salts and other nutrients [5]. Oxygen is sparingly soluble in aqueous solutions, a limitation which is exacerbated by factors such as salinity and culture viscosity [6]. High-cell density cultures are highly viscous which limits the diffusivity of oxygen and causing a steep decline in dissolved oxygen (DO) [5]. The increase in culture viscosity is more severe in bioprocesses in which high molecular weight (MW) biopolymers are produced in the extracellular environment.

Limitations of oxygen mass transfer in fermentation can be solved by increasing agitation, improving aeration or using auxiliary liquids which are immiscible in the aqueous phase [7-9]. Enhancing agitation and aeration can boost up the HA yield markedly compared with the corresponding anaerobic culture [10, 11], while too high an agitator speed would cause cell damage and lead to a drop in the HA yield subsequently [10], resulting in a higher cost for the energy consumption in the meantime. Additionally, utilizing pure oxygen for aeration can also be detrimental to the cell metabolism. An alternate approach to influencing oxygen transfer rates (OTRs) is in the addition of water-insoluble compounds which possess a strong affinity for oxygen (referred to as oxygen vectors) [12, 13], a technique that has been applied successfully to lab-scale studies over the last few decades [14]. The limiting step in the aerobic

biological processes is low solubility of oxygen in aqueous growth media which can be improved by the usage of the oxygen vectors [15, 16]. Larger local oxygen concentration gradients will be created in the bulk continuous phase by shuttling of oxygen-rich vector droplets from the gas-liquid interface to the bulk liquid due to the presence of oxygen vectors in system, and meanwhile, the surface tension (σ) at the air-water interface can be decreased leading to reduced bubble coalescence and, in turn, smaller air bubble diameter and increased interfacial area (a) for mass transfer. Additionally, water-insoluble vector droplets can collide with and break air bubbles resulting in reduced bubble size [17, 18]. The criteria for choosing a vector must involve a high affinity for oxygen to dissolve, immiscibility with liquid phase, no toxicity and inhibition of microbial activity, non-biodegradability in the presence of primary carbon sources, non-volatility in operating condition, and reasonably low cost [19]. The selection of an proper vector can potentially reduce operating costs associated with power consumption from high agitation rates and compressed air delivery, oxidative stress resulting from exposure to oxygen hot spots in the vicinity of spargers when supplemental oxygen is used [20, 21], and excessive foaming observed during high-cell density bacterial cultivations [19].

In the context of a system containing a dispersed phase (liquid oxygen vector), continuous phase (aqueous media), gas phase (air) and suspended bacterial cells, there are five possible pathways for oxygen transfer from gas bubbles to bacterial cells, which increases the opportunity for oxygen to get into the cells. New interfacial areas will be established, and the transfer of oxygen from gas bubble to cells may be enhanced by a high-performance gas/vector/liquid/cell pathway [17]. Oxygen vectors have been widely utilized to the enhance

the production of HA in Streptococcus zooepidemicus cultures [22], poly(γ-glutamic acid) in *B. subtilis* cultures [23], ε-poly-lysine in *Streptomyces albulus* cultures [24], a continuous toluene degradation process in *Pseudomonas putida* DOT-T1E cultures [17] and recombinant protein expressed in *Escherichia coli* [25].

1.2 Research objective

The overall objectives of this thesis were to:

1) compare various HCs and PFCs as oxygen vectors in terms of cell density, HA titer, MW and changes in levels of dissolved oxygen;
2) compare the performance of culture with selected oxygen vectors from 1) different concentration and different adding time to obtain the optimal conditions for each vector supported by oxygen mass transfer efficiency (k_La);
3) evaluate HA production in recombinant *B. subtilis*, under higher agitation rate with/without positive vectors at optimal concentration, in terms of its titer and MW and compare with lower agitation rate with supplemental oxygen to maintain the DO concentration at 20 ± 5% saturation.

1.3 Outline of thesis

Chapter 2 is a review of hyaluronic acid biosynthesis pathway in *B. subtilis*; basic theories of mass transfer in a gas-liquid surface and measurements of oxygen mass transfer coefficients (k_La) and approaches to modelling mass transfer in bioreactors; different bubble regimes properties; various design of bioreactors and their suitable platforms to be used; and a systemic overview of oxygen vectors including its categories, transfer pathways in a bioreactor system, spreading properties of different kinds of liquid oxygen vectors, the mechanism of

enhancement to oxygen mass transfer caused by oxygen vectors and application to bacterial cultivations using oxygen vectors for improvements. In Chapter 3, various liquid oxygen vectors and different operating conditions are assessed and compared in conventional stirred tank reactor (STR) for production of HA in *B. subtilis*. The comparison involves: 1) various kinds of HCs and PFCs as vectors, 2) different adding time and concentration of several selected vectors, and 3) the products under high agitation rate combined with positive HC and PFC vectors. Finally, Chapter 4 summarizes the results from the investigation presented in Chapter 3 and implications to the biochemical industry, and proposes future studies to usage of proper oxygen vectors to obtain the improvements of the quality and quantity of bioproducts.

Chapter 2- Literature Review

2.1 Hyaluronic acid biosynthesis pathway

HA is synthesized by the polymerization of the monosaccharides from the two nucleotide sugars UDP-glucuronic acid (UDP-GlcUA) and UDP-*N*-acetylglucosamine (UDP-GlcNAc) [2]. The enzyme that catalyzes this reaction is HA synthase or HAS. Production of HA in a recombinant host was first proposed and demonstrated in *B. subtilis*, resulting in the exploration of heterologous HA production in several other organisms [3]. As both *Streptococcus* sp. and *B. subtilis* are Gram-positive microorganisms, HA biosynthesis pathways can be readily adapted to achieve production in *B. subtilis* (Figure 1). The only enzyme *B. subtilis* lacks is the hyaluronan synthase, which is encoded by the *hasA* gene [2]. Initially beginning with glucose as a carbon source, two parallel metabolic branches can be established which eventually, through multiple sugar intermediates, culminate in the synthesis of the two nucleotide sugar substrates, UDP-GlcUA and UDP-GlcNAc [1]. HA production is a metabolic process requiring 2 mol of glucose, 5 mol of nucleoside triphosphates (3 as ATP and 2 as UTP), and 1 mol acetyl-Coenzyme A for every polymer subunit (i.e. -GlcUA-GlcNAc-) synthesized. HA producing *Streptococci* have evolved a dedicated expression system to address this issue, which entails expression of *has* genes to maintain suitable precursor flux during HA capsule formation [2]. In addition to *hasA* (encoding HAS), *S. pyogenes* expresses *hasB* (*tuaD*), encoding a UDP-glucose 6-dehydrogenase, and *hasC* (*gtaB*), encoding a UTP-glucose-1-P uridylyltransferase, while *S. equisimilis* also expresses *hasD* (*gcaD*), which encodes a UDP-GlcNAc pyrophosphorylase [2]. Thus, the evolved expression system in these streptococcal species via operons ensures that abundant levels of various precursor sugars are available to support both

HA biosynthesis and cell growth [1]. Accordingly, *B. subtilis* has homologues to the *hasB*, *hasC*, and *hasD* genes, and they are designated *tuaD*, *gtaB*, and *gcaD*, respectively. Artificial operons were therefore constructed which contained the *hasA* gene from *Streptococcus* together with one or more of these latter *B. subtilis*-derived genes to be introduced into the new HA synthesis host system.

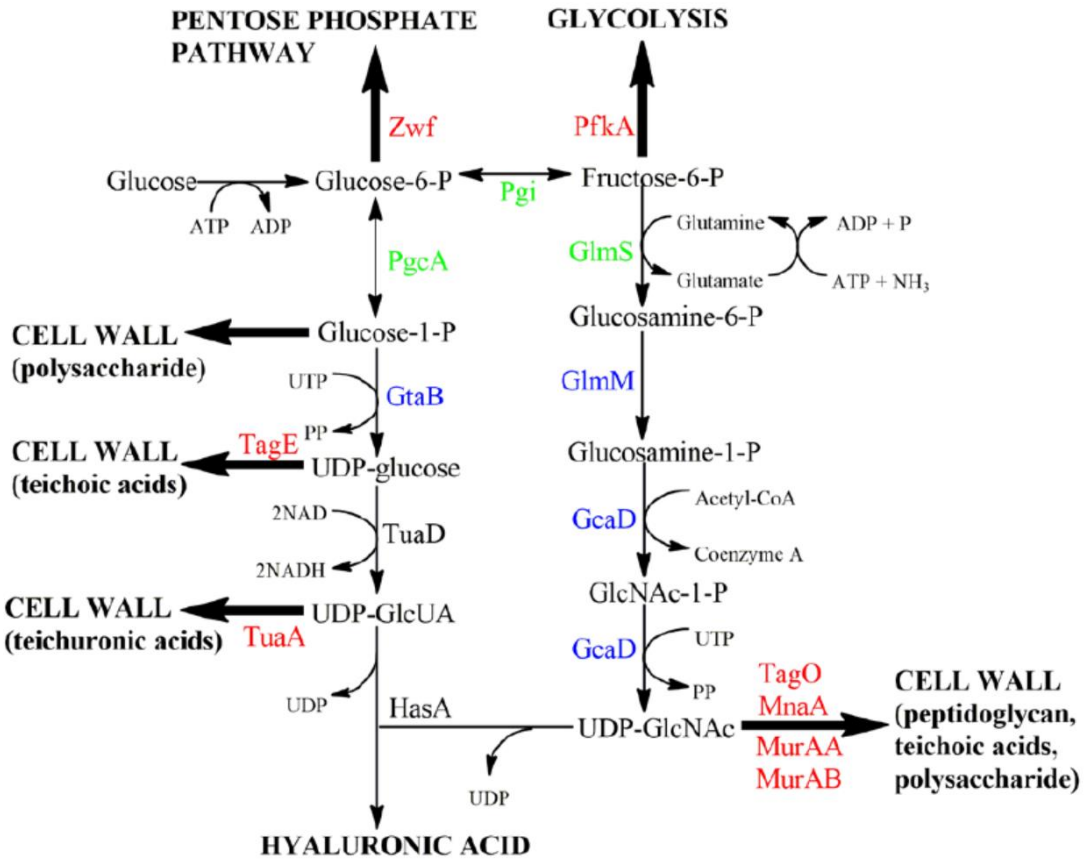

Figure 1: HA biosynthetic pathway in *B. subtilis.* Enzymes in black text are prerequisite for HA production. Enzyme names listed by category: TuaD, UDP-glucose 6-dehydrogenase; HasA, hyaluronan synthase; Pgi, glucose-6-P isomerase; PgcA, phosphoglucomutase; GlmS, glutamine-fructose-6-P amidotransferase; GtaB, UTP-glucose-1-P uridylyltransferase; GlmM, phosphoglucosamine mutase; GcaD, UDP-GlcNAc pyrophosphorylase; Zwf, glucose-6-P 1-dehydrogenase; PfkA, 6-

phosphofructokinase; TagE, UDP-glucose:polyglycerol phosphate glucosyltransferase; TuaA, putative undecaprenyl-phosphate N-acetylgalactosaminyl-1-P transferase; TagO, UDP-GlcNAc: undecaprenyl-P N-acetylglucosaminyl-1-P transferase; MnaA, UDP-N-acetylmannosamine (ManNAc) 2-epimerase; MurAA, UDP-GlcNAc 1-carboxyvinyltransferase; MurAB, UDP-GlcNAc 1-carboxyvinyltransferase. Adapted from [2].

2.2 Mass transfer

2.2.1 Mass transfer theories

Multiple theories for mass transfer between a gas and a liquid have been proposed and developed. The two main theories are two-film theory and penetration theory. According to the two film theory, molecules have to move through two thin films which exist on either side of an interface separating respective bulk phases [26, 27] (Figure 2A). There is a resistance that results in a concentration gradient associated with each step [27]. The assumption is that a region exists in which steady state transfer is occurring [27, 28]. Compared with the two-film theory, penetration theory indicates that molecules within the gas phase existing as randomly moving clusters will come close to contact the interface for a fixed amount of time. During this finite contact time, some of the molecules within the clusters penetrate the interface, entering the liquid phase. Following separation, the molecules in the clusters mix back into the gas bulk [29] (Figure 2B). The assumption is that the interface is constantly altering as clusters of molecules move into and out of contact with the interface [28, 29]. It has been proved that neither of the aforementioned theories is completely valid for every situation [30]. As such, a combination of the two theories called the film-penetration theory was developed [28]. In

simple terms, when an interface is developing, the assumption of a changing interface (i.e., penetration theory) applies, and once the interface is completely established, a film will be maintained under steady-state conditions (i.e., two-film theory applied) [28] (Figure 2C).

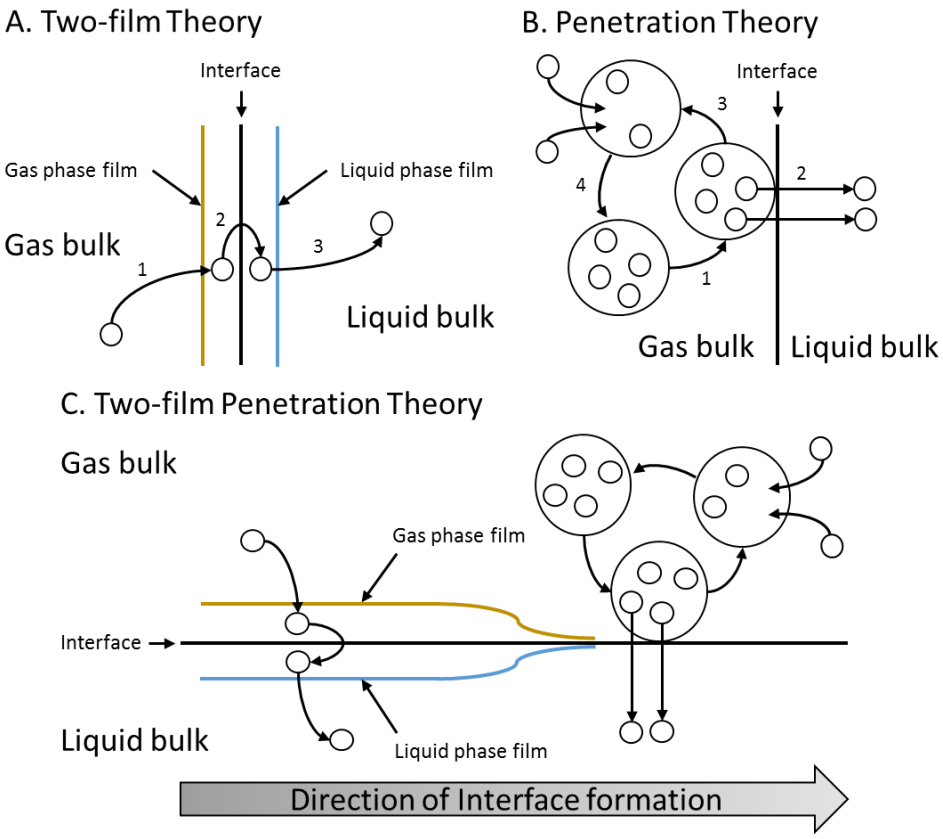

Figure 2: Overview of mass transfer theories used for prediction of OTR in biological cultivations.

A) Two-film theory: 1. Molecules within the gas bulk enter the gas phase film 2. Molecules within the gas film cross the interface into the liquid phase film 3. Molecules exit from within the liquid phase film enter the liquid bulk.

B) Penetration theory: 1. A cluster of molecules within the gas bulk contact with the gas-liquid interface 2. Some molecules within the cluster cross the interface into the liquid bulk 3. The

remaining molecules within the cluster detach from the interface re-entering the gas bulk 4. New molecules within the gas bulk enter the cluster, repeating the cycle.

C) Two-film penetration theory: as an interface forms between the gas bulk and liquid bulk molecules initially cross the interface following the penetration theory. As the interface has been established, molecules cross the films between interface following the two-film theory.

2.2.2 Oxygen mass transfer in bioreactors

The selection of bioreactors is a critical step in the development of any commercially feasible bioprocess, particularly when microbial expression hosts are applied owing to the high oxygen demand and viscous nature of fully developed cultures. The STR has been the default choice for cultivation of aerobic bacteria due to superior mass transfer and flexibility in terms of operating conditions (i.e., temperature, pH, air flow, agitation, and pressure). Understanding the mechanism of oxygen mass transfer and response to fermentation parameters ensures appropriate bioreactor selection to achieve target yields.

Under conditions typical for aerobic cultivation of unicellular microbes, the rate of oxygen diffusion into the liquid film adjacent the gas-liquid interface controls the overall rate of oxygen transfer, which is called liquid film control.

In general, the oxygen transfer rate (OTR) is derived from the simple two-film model in which resistance exists as a thin film occurring on either side of the gas-liquid interface. Equation 1 is obtained by assuming mass transfer resistance is negligible on the gas side of the interface:

$$OTR = \frac{dC_L}{dt} = k_L a(C^* - C_L) \quad (1)$$

where k_La, the volumetric mass transfer coefficient, is the product of the local mass transfer coefficient (k_L) and interfacial area (a); C^* is the bulk liquid saturation concentration of oxygen; and C_L is the bulk liquid concentration of oxygen versus time (t) [31]. Mass transfer is driven by the concentration gradient between the interface and bulk liquid. The concentration gradient is affected by cellular oxygen uptake rate and solubility, the latter being a function of temperature, salinity, and pressure [27].

Considerable efforts have been made to develop empirical correlations for k_La based on parameters such as power input per unit volume (P/V), liquid effective viscosity (μ_e), and superficial gas velocity (V_s) [27]:

$$k_La = AV_s^a \left(\frac{P}{V}\right)^b \mu_e^c \quad (2)$$

The exponents found in Equation 2 vary significantly between studies, for example, [32-34], owing largely to experimental techniques used to measure k_La [34] and inherent difficulty in obtaining reproducible estimates. Alternatively, some correlations replace P/V with stirrer speed, N [35-37], while others make use of dimensionless variables such as the Reynolds ($\rho NT/\mu_e$), Schmidt ($\mu_e/\rho D$), and Weber ($\rho N^2T^3/\sigma$) numbers to evaluate k_La via the Sherwood number, k_LaT^2/D, where T is the stirrer diameter, ρ is fluid density, D is the oxygen diffusivity in liquid, and σ is the interfacial tension [38-40].

A theoretical approach has also been used to determine k_La based on Higbie's penetration theory [41], which estimates k_L via the exposure time (t_e) for mass transfer represented by the ratio of the Kolmogorov length scale, $\eta = (v^3/\varepsilon)^{0.25}$, and fluctuation velocity, $u = (v\varepsilon)^{0.25}$, of turbulent eddies [42] where v is the kinematic viscosity and ε is the energy dissipation rate of turbulence:

$$k_L = 2\sqrt{\frac{D}{\pi t_e}} = 2\left(\frac{D}{\pi}\right)^{1/2}\left(\frac{\varepsilon}{\nu}\right)^{1/4} \quad (3)$$

A theoretical basis for k_La determination is controversial due to inconsistency between empirical correlations obtained under similar conditions, and the simplified approach in which dependencies on reactor geometrical parameters are lumped together (i.e., constant A in Equation 2). Theoretical models will provide a better understanding of the relationships between process parameters and k_La, reducing the difficulties inherent to bioreactor scale-up, a complicated process which is highly dependent on maintaining acceptable mass transfer. Sensitivity analyses and optimization could facilitate bioreactor performance and process efficiency, particularly when interactions between V_s and N are considered. Qualitatively, k_La is controlled by mechanical agitation for $N>N_c$ (agitation controlled), where N_c is the critical impeller speed, ignoring the effect of aeration [36, 43]. Similarly, under vigorous aeration and $N<N_c$, agitation has a negligible effect on k_La (bubbling controlled) [36]. A previous study elucidated that constants associated with V_s and N in standard correlations vary significantly across the intermediate regime [36]. Consequently, operation in the intermediate regime (the most common situation) would be most efficient under optimized conditions based on consideration of expression host, sensitivity of product to oxidation, relative utility and process gas costs, etc.

2.3 Bubble regime properties

There are five forms for the flow of bubbles within a liquid phase, referred to as bubble regimens, depending on bubble size and distribution. Under the homogenous regime: 1) perfect bubbly and 2) imperfect bubbly; under the heterogeneous regime: 3) churn flow, 4) slug flow and 5) annular flow (Figure 3) [44, 45]. Different flow regimes can be obtained by altering the

superficial gas velocity (V_s) [45, 46]. V_s is defined as the gas flow rate through the liquid phase divided by the cross sectional area [45, 46]. Additionally, alterations to V_s correlate with changes in gas holdup (ϕ), which ϕ is defined as the volume fraction of the liquid phase occupied by gas bubbles in the bulk liquid [45, 46].

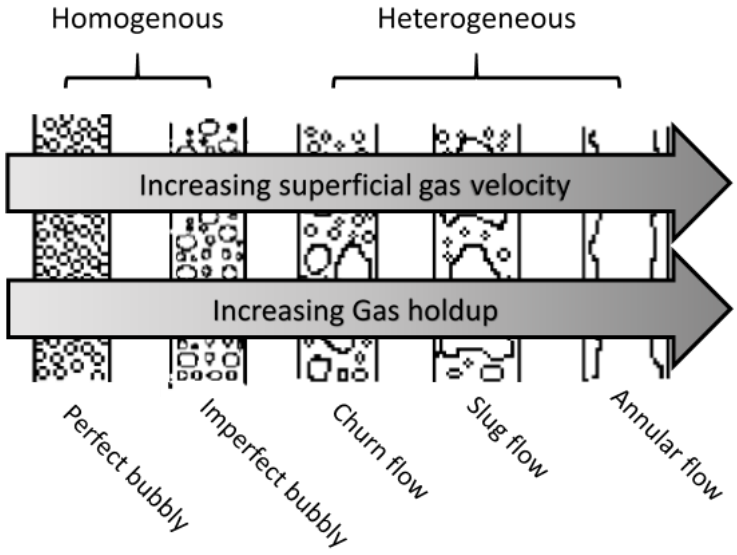

Figure 3: Schematic representation of the five different bubble regimes: homogenous-perfect bubbly and imperfect bubbly; heterogeneous-churn flow, slug flow and annular flow. The arrows indicate the direction of increasing superficial gas velocity and increasing gas holdup. Adapted from [47] and [44].

Perfect bubbly and imperfect bubbly regimes are characterized by a homogenous distribution [48] of small bubbles with lower rise velocities [49], minimal bubble coalescence or break-up [50], and a linear increasing relationship with V_s [51]. Churn-flow is described as having a heterogeneous bubble size distribution with larger bubbles forming via coalescence [49]. The formation and dissipation of bubbles generates turbulence which creates a mixing effect in the liquid bulk [48], and results in lower k_L values compared to homogenous bubbly regimes [45]. Due to the mixing effects associated with this regime, it is commonly used in

industrial size column reactors [48, 52]. Slug flow is only observed in small diameter column reactors and is characterized by large bubbles being stabilized by the walls of the reactor [45]. Annular flow is only achievable at very high V_s and is characterized by the liquid phase existing as a film on the walls of the column with the gas phase occupying the interior [44, 46]. A transitional stage exists as bubbles transfer from homogenous to heterogeneous flow regimes [45]. In a mass transfer limited situation, such as biological cultivation, the ideal bubble regime will maximize the number of small diameter bubbles and maintain liquid phase mixing, which can also enhance the mass transfer by increasing interfacial area.

2.4 Biological Reactors

There are three main types of liquid based reactors used for biological fermentations (i.e., stirred tank (STR), bubble column, and airlift reactors) (Figure 4). The selection of a reactor type is dependent on several criteria: the size of reactor required, cost, cultivation media viscosity, physiology of the biocatalyst and mass transfer requirements [53, 54]. When the working volume is over 500 m^3, STRs start to encounter mechanical issues due to power requirements greater than 1 MW [53]. When the working volumes are quite large like wastewater treatment, airlift reactors (e.g., activated sludge reactors) are top priority over bubble columns due to their merits in substrate addition control [53]. For high viscosity cultures STRs are commonly utilized as airlift and bubble columns fail to work properly under this condition [53]. Therefore, high viscosity cultivations are only scaled to a maximum volume of 500 m^3. For low viscosity fermentations with volumes >500 m^3, bubble columns are used, while airlift reactors are employed for volumes <500 m^3 [53]. Every biocatalyst possesses specialized physiology to carry out biochemical reactions efficiently. As a result, optimized conditions

(operating conditions for the reactor) that maximize a target metabolites' production are determined by a given biocatalyst. Sheer sensitive organisms or products are not recommended to be processed in STRs owing to an elevated sheer force associated with mechanical mixing [54]. The appropriate nutrient levels, acceptable heat and sufficient mass transfer provided during the cultivations ensure the stabilized biocatalyst performance. It is achievable to optimize oxygen mass transfer (the limiting process variable) through manipulation of design parameters according to different types of reactors.

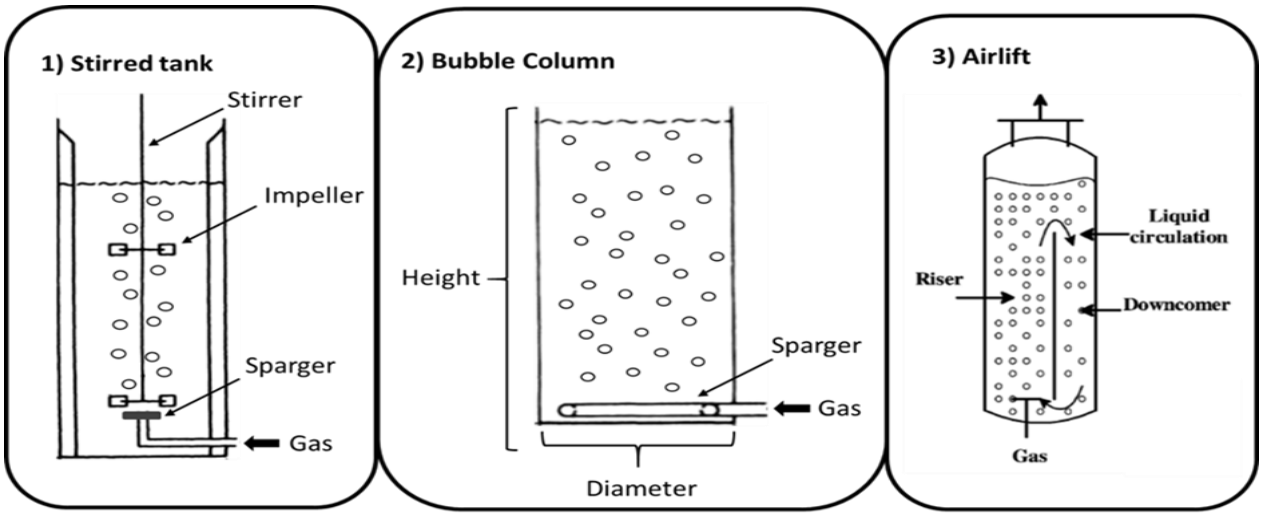

Figure 4: Basic design for three different reactor types used for biological cultivations. Adapted from [53] and [47].

2.4.1 STRs

The gas mixing within STRs is predominantly generated by a stirrer mechanically with attached impellers [27]. Therefore, the mixing associated with pneumatical processes becomes a minor consideration refer to bubble columns and airlift reactors, and the STRs are designed to minimize bubble diameter. Under a sufficient agitation speed (measured in revolutions per min; rpm), impellers are capable to create additional smaller diameter bubbles by physically

colliding with and splitting larger bubbles [55]. Mechanical splitting of bubbles allows for a higher aeration rate to be used while maintaining high numbers of small bubbles [55]. The STRs can provide high mass transfer efficiency due to the mechanical mixing and the bubble splitting [53]. Thus, mass transfer rates are affected by the stirrer design, which encompasses the selection of impeller number and spacing, and blade shape and angle [53]. In addition to bubble size, impeller type and speed influence V_s and ϕ. Theoretically, V_s should be unaffected by impeller speed as reductions in bubble size are counteracted by the lower rise velocity of smaller bubbles resulting in the same overall flow [56]. However, the air bubbles are likely to escape from the impeller zone due to variations in local gas velocity resulting from an imbalance between impeller speed and gas flow rate [56]. Based on observations about bubble size and V_s, the ϕ increases with impeller speed [57], as does the k_La with the additional impellers and elevated agitation rate [58, 59].

2.4.2 Bubble columns and airlift reactors

Bubble column reactors are based on the pneumatic systems for agitation and gas mixing [27, 53]. Accordingly, designing and modifying the geometric properties to pursue elevated OTRs is limited to changing column dimensions and using different types of gas spargers. With increasing the column diameter, ϕ was shown to decrease through bubble-wall interactions in small diameter columns (≤10cm) [60, 61]. Column diameters (>10-15cm), were observed to have an insignificant effect on ϕ [62]. Smaller bubble ϕ is not influenced markedly by increasing the column diameter, while larger bubble ϕ decreases with increasing diameter [63-65]. Column height and aspect ratios were proved to have no effect on ϕ above 1-3 m and 5,

respectively [66]. The types of gas spargers are determined for the bubble size entering the columns, thus, smaller orifice diameters yield smaller bubbles leading to an increase in ϕ [67]. Additionally, the types of gas distributors impact the ϕ [66].

Airlift reactors are different from bubble columns by utilizing loops and hydrostatic pressure differences to circulate the fluid [47]. Smaller air bubbles enable to circulate within the liquid resulting in longer residence times and higher mass transfer rates within airlift reactors [47], which is particularly an suitable candidate for industrial sewage treatment.

2.5 Oxygen vectors

2.5.1 Oxygen vector categories

Oxygen vectors are water-immiscible compounds (solid or liquid phase) that typically have a greater capacity to dissolve oxygen compared to aqueous media solutions. Hydrocarbons (HCs) [19, 68-70], perfluorocarbons (PFCs) [22, 71, 72], vegetable oil [73] and silicone oil [17, 19] have been applied to enhancing OTRs as liquid oxygen vectors, while solids polymers such as silicone rubber [19, 74], nylon [75], glass beads [75], Hytrel [19], Kraton [19], Desmopan [17, 19] and Elvax [17] have also provided improved mass transfer in stirred-tank reactors (STRs). HCs have been utilized extensively as liquid oxygen vectors in bacterial cultivations (simulated or otherwise) [11, 19, 23, 24, 69-71, 76, 77], while PFCs promise to be functional as next generation oxygen vectors due to their substantially higher oxygen solubility, lower γ and satisfied biocompatibility [78]. The enhancement in solubility of oxygen in PFCs can be attributed to their intermolecular arrangement, rather than F-O electrostatic interactions, which has been confirmed by several studies of paramagnetic relaxation induced by the presence of

oxygen in PFCs and HCs. The longitudinal relaxation time (T_1) corresponds to the process of establishing (or re-establishing) the normal Gaussian population distribution of α and β spin states in a magnetic field [79]. Nuclear relaxation arises from a dipolar interaction between the electron spins of oxygen and spins of the solvent nuclei (either F or C in this case) modulated by molecular motion [80]. T_1 can be related to the mole fraction of solute (x_G) by Equation 8:

$$\frac{1}{T_1} - \frac{1}{T_1^0} = q_x x_G \tag{4}$$

Where T_1^0 is the relaxation time of the pure solvent and q_x is the relaxation coefficient [80, 81]. PFCs commonly present lower q_x values compared to their parent HCs (e.g., 60 and 40 s^{-1} for benzene and perfluorobenzene, respectively), such that an inverse (roughly linear) relationship between q_x and oxygen solubility exists [80, 82]. Relaxation rates (LHS of Equation 8) in HC systems can result from a continuous translational diffusion of oxygen through the network of HC molecules. Conversely, a discontinuous diffusion model of oxygen molecules in PFCs has been proposed, in which a network of solvent molecules would enclose a cavity where oxygen molecules are temporarily trapped prior to migrating into an adjacent cavity [80, 82]. The relatively large size of fluorine atoms in PFCs (compared to hydrogen atoms in HCs) leading to irregular molecular arrangements, and, in turn, opening large cavities for oxygen entrapment, is a reasonable picture of the action of PFCs when dissolving large quantities of gaseous molecules, given the lower boiling points and higher viscosities of PFCs versus HCs [82].

The enhancement in OTRs via solid vectors is thought to occur through 1) elevated turbulence at the gas-water interface through particle-stagnant film collision and mechanical

disruption simultaneously reducing the gas bubble sizes, and/or 2) the shuttling effect which entails that particles saturated with oxygen at the gas-water interface moving into the bulk liquid where the oxygen is desorbed (regenerating the particle for subsequent transfer) [19, 83]. The effectiveness factor (*EF*) has been used to evaluate the performance of oxygen vectors [19]:

$$EF = \left(\frac{OTR_{VW}}{OTR_W} - 1\right) \times 100\% \quad (5)$$

Even though certain solid vectors possess high affinities for oxygen, they still provide lower values of *EF* than those vectors with significantly lower (in some cases negligible) affinity. The equilibrium concentration of oxygen in the combined liquid phase (C^*_{mix}) was used to evaluate enhancements to the concentration gradient driving mass transfer:

$$C^*_{mix} = f_W \frac{C_G}{K_{GW}} + f_V \frac{C_G}{K_{GV}} \quad (6)$$

Where f_i is the volume fraction of respective phases, C_G is the concentration of gaseous oxygen and K_{ij} represents the partitioning coefficients between respective phases. Kraton and Desmopan provided increases of 220% and 175%, respectively, to the concentration gradient available for mass transfer (based on relative C^*_{mix} values), while respective *EF* values for Kraton and Desmopan were 23% and 171% [19]. Similarly, glass beads (D_{oxygen}<1x10^{-15} cm^2/s) and nylon (D_{oxygen}=1.6x10^{-9} cm^2/s) provided significant enhancements to the k_La, while silicone rubber (D_{oxygen}=3.4x10^{-5} cm^2/s) and a styrene-butadiene copolymer (D_{oxygen}=1.4x10^{-6} cm^2/s) caused a reduction to the k_La in a STR [84]. The reduce in k_La values was likely owing to an increase in the time needed to reach oxygen saturation in the bulk liquid in the presence of silicone rubber (i.e., the vector was absorbing the oxygen), as the OTR in this dispersed system

was significantly higher compared to that without vector. Accordingly, the work completed to date indicates that the selection of solid vectors is a complicated process for the reason that the oxygen affinity of a given material should not be the only concern and they will not promise a higher OTR such as the evident from Kraton.

2.5.2 Pathways of mass transfer

In the context of a system containing a dispersed phase (liquid vector), continuous phase (aqueous media), gas phase (air) and suspended bacterial cells, there are five possible pathways for oxygen transfer from gas bubbles to bacterial cells as presented below (Figure 5) [71].

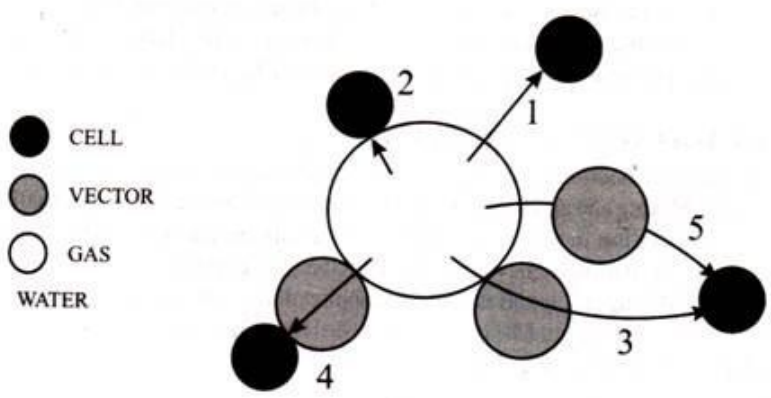

Figure 5: Possible pathways for oxygen transfer from gas bubbles to bacterial cells in aqueous cultivation media containing an oxygen vector.

Liquid vectors are often categorized based on their propensity to form droplets (beading) or films (spreading) when contacting an aqueous phase. For spreading liquid vectors, parallel transfer is the most likely pathway for oxygen transfer (i.e., simultaneous gas-water and gas-vector oxygen transfer) [70, 71]. However, mass transfer in series (i.e., gas-vector-water or gas-water-vector oxygen transfer) was determined to be the most essential pathway in vector-

water systems [85], and the significantly higher k_L values for gas-vector compared to gas-water oxygen transfer for spreading vectors (and highly similar k_L for vector-water and gas-water) indicate that mass transfer occurs in series by the gas-vector-water pathway (then taken up by the bacterial cells) [71]. In addition, the significantly reduced σ between gas and vector relative to gas and the aqueous phase favors gas-vector transfer by reducing the local free energy [86]. A qualitative representation of the oxygen transfer profile is shown below (Figure 6).

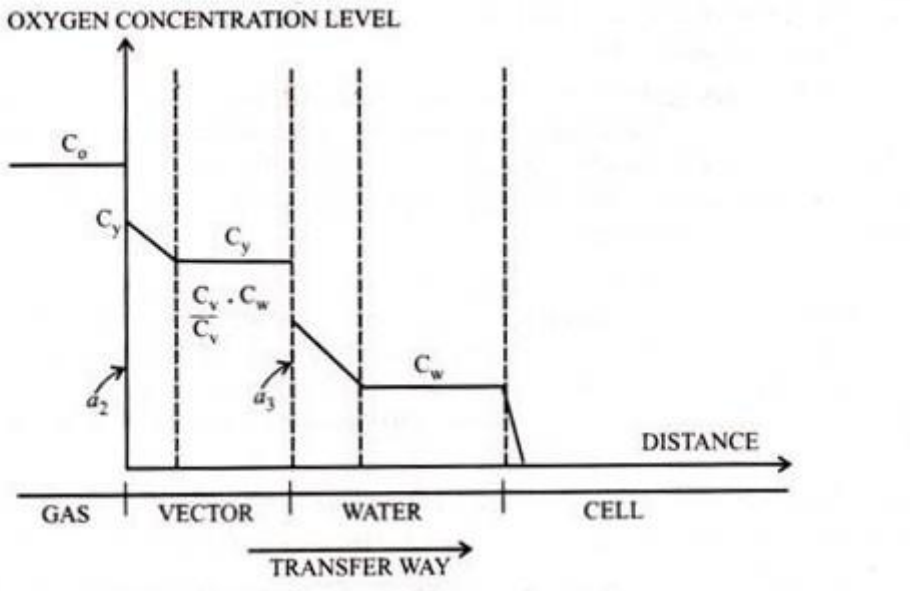

Figure 6: Profile of oxygen transfer in cultivation media containing a spreading oxygen vector. a2 and a3 represent the gas-vector and vector-water interfacial areas. Adapted from [71].

'Coalescence' of gas bubbles and vector (n-dodecane or forane) droplets has been observed in a static aqueous system [71], confirming that gas-vector mass transfer is a possible scenario. Gas-vector coalescence has also been observed in dynamic experiments in which toluene, dodecane or refined petrol were injected into a water stream containing a fixed number

of stationary gas bubbles [87]. The formation of gas-vector complexes can be addressed from the point of view of a change in surface energy (E_S):

$$\Delta E_S = 4\pi([\sigma_{GV}R_b^2 + \sigma_{VW}R_c^2] - \sigma_{VW}R_d^2 - \sigma_{GW}R_b^2) \quad (7)$$

Where R_b, R_c and R_d represent the radii of the gas bubble, gas-vector complex and vector droplet, respectively. If the vector droplet is much smaller than the gas bubble (which can be achieved mechanically), then $R_c \approx R_b$, and the following condition of the bubble-to-droplet size ratio supporting gas-vector coalescence (i.e., $\Delta E_S < 0$) can be derived from Equation 8:

$$\left(\frac{R_b}{R_d}\right)^2 < \frac{\sigma_{OW}^*}{\sigma_{OW}^* + \sigma_{OG}^* - \sigma_{WG}^*} = \frac{\sigma_{OW}^*}{-S^*} \quad (8)$$

Where * indicates properties of a mutually saturated system (for $S^* < 0$) and S^* refers to spreading coefficient. For $S^* > 0$, gas-vector coalescence would be favorable for any size ratio [87]. One additional criterion must be met to attain vector film formation over droplet separation, in addition to Equation 8, which is the minimum vector film thickness (2-10 nm) [88].

2.5.3 Spreading coefficient

The spreading characteristics of oxygen vectors can determine the path(s) and efficiency of oxygen transfer in biological cultivations. There are two pathways for oxygen mass transfer between dispersed oxygen vectors and dispersed gas phases: 1) direct gas/vector contact and 2) indirect mass transfer through the intermediate continuous aqueous phase. The effect of adding a second water-immiscible liquid phase (i.e. oxygen vector) may thus be expected to be different depending on the spreading coefficient *S*, defined as:

$$S_{VW} = \sigma_{WG} - (\sigma_{VG} + \sigma_{VW}) \quad (9)$$

where σ_{WG}, σ_{VG}, and σ_{VW} are the water-gas, vector-gas, and vector-water interfacial tensions, respectively. For spreading vectors [(S_{vw})>0], oxygen transfer between air and vector can occur as the vector spreads around air bubbles [85, 89], resulting in improved oxygen transfer due to large concentration gradients between the vector and aqueous medium and reduced air bubble diameter as the vector disrupts coalescence [17, 18]. Direct contact is thus likely and high oxygen mass transfer coefficients are expected (see Figure 7).

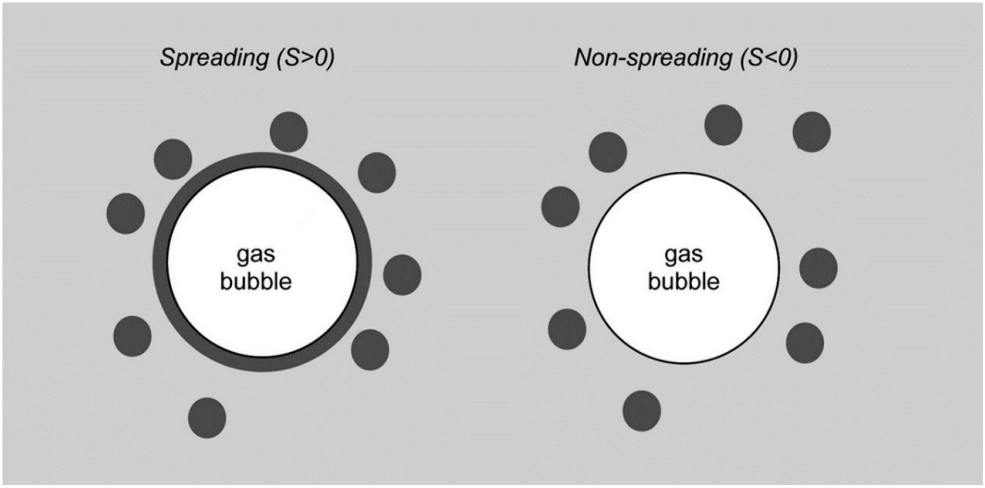

Figure 7: Effect of spreading coefficient over the mass transfer pathway in a vector-in-water emulsion. Backgrounds: continuous phase (water/media); Circles: dispersed phase (oxygen vectors).

When the spreading coefficient is negative, on the other hand, such an organic film will be thermodynamically not stable. Mass transfer between gas and oxygen vector is indirect through the aqueous phase, involving additional mass transfer resistances (see Figure 7). For non-spreading vectors [(S_{vw})<0], oil droplets may enhance oxygen transfer by 1) disturbing the boundary layer around an air bubble, or 2) making direct contact with the air bubble, and subsequently releasing oxygen into the bulk phase [90]. Thus, oxygen mass transfer

enhancement may still occur due to the existence of oxygen vector droplets which are much smaller than the bubbles, typically~50 μm, in the bubble boundary layer. They may either improve the concentration gradient due to a shuttle effect or improve boundary layer mixing and diffusion of oxygen due to the hydrodynamic effect. However, the accumulation of vector droplets at the bubble surface may impede oxygen transfer [91], and direct contact between air and vector may not occur without sufficient agitation or if the S_{vw} is not approaching 0 [7]. It shows very clearly that mass transfer coefficient increases with stirrer speed and gas flow rate. Accordingly, oxygen transfer in cultures containing non-spreading vectors may proceed in the order air-medium-vector or may simply bypass the vector altogether [92]. Estimates of the S_{vw} vary widely for different hydrocarbons and are sparsely available for perfluorocarbons. For example, the S_{vw} (25 °C) reported for n-dodecane ranges between -5.9 [7] and 3.7 [93], such that accurate prediction of spreading behavior may be difficult. In general, the S_{vw} decreases with increasing size and branching/methylation of the vector molecule [7, 94, 95], and the S_{vw} increases with increasing temperature [95, 96] and aqueous glucose concentration [97].

At present, two rudimentary mechanisms for non-spreading vectors have been proposed, one is grazing or shuttle effect [98]and the other hydrodynamic effect [99, 100]. According to shuttle effect, small dispersed particles move around frequently and randomly between the stagnant mass transfer zone near/at the gas-liquid interface and the liquid bulk due to the bulk circulation. Near/at the interface the gas solute is adsorbed/absorbed on/in dispersed particles, and local concentration gradient increases resulting in the enhancement of gas absorption. Hydrodynamic effect is proposed firstly mainly for bubble systems (stirred tanks, bubble columns). According to this effect the presence of dispersed particles can influence the

hydrodynamic behavior of three-phase systems. Particles will collide and interact with the gas-liquid interface or may cause turbulence near/at the gas-liquid interface, leading to the appearance of smaller effective diffusion layer. Accordingly, diffusion of gas into the liquid film and mixing of gas into the bulk liquid can be improved by dispersed particles, with k_L being increased. There is a thin layer of liquid film wrapping the particles dispersed in bulk liquid as shown (in Figure 8). The gas solute molecules need go through this stagnant liquid film which is more ordered than liquid bulk by molecular diffusion to reach adsorptive particles and then diffuse and mix into the bulk liquid.[83]

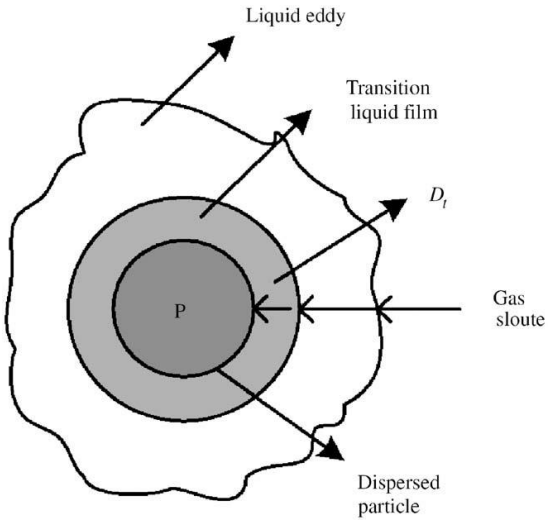

Figure 8: The sketch of the dispersed particles in continuous liquid phase.

2.5.4 Enhancements to mass transfer

The presence of the dispersed phase may influence gas-liquid mass transfer in two basic ways: the existence of oxygen vector may alter the specific interfacial area available for oxygen mass transfer or it may affect the rate of oxygen flux across the gas-liquid interface. Changes in the gas-liquid interfacial area occur when the oxygen vector alters the gas-liquid interfacial tension in the system or when the dispersed droplets affect bubble breakup or coalescence. The effect

of oxygen vectors on interfacial area (a) in gas-vector-water systems is poorly understood. It has been reported that small increases in a arise from the prevention of gas bubble coalescence for low f_V values (dispersed toluene), while a decreases as f_V increases further due to reduced turbulence [101, 102]. Dispersed dodecane, heptane and 1-octanol decreased a as f_V increased without achieving a maxima value [37]. Conversely, a 15% decrease in the bubble Sauter mean diameter was observed for a n-dodecane dispersed system for $f_V = 0.23$ (also corresponding to the maximum k_La), representing a proportional increase in a [71]. Increasing f_V further resulted in a reduction in the k_La, suggesting that a similar reduction in a may have resulted from exceeding the optimal f_V value which was not observed in some cases [37]. Conversely, dispersed FC-40 (PFC) had no significant effect on a for f_V up to 0.15, although the OTR steadily increased with f_V up to a value of 0.4 [85]. Therefore, the evident indicates that there is no consensus on the effects of liquid vectors on a, and further investigations are required to address this issue. The impact of solid vectors on a has not been studied in detail, however, a reduction in a is expected due to direct mechanical bubble breakage [19]. Alternatively, changes in the rate of solute flux across the gas-liquid interface occur when the oxygen vectors alter either the liquid film hydrodynamics or the solute permeability.

As discussed for solid vectors, the k_La may not completely represent the utility of an oxygen vector for enhancing oxygen availability in bacterial cultivations, as the initial loading of the vector may extend the time required to reach saturation in the bulk liquid. Moreover, reports of the effect of the dispersed phase on the k_La are at times inconsistent, as is the case with estimation of a. For example, dodecane was reported to enhance k_La slightly up to $f_V \approx 0.01$ after which a decline was observed [102], while the k_La increased ≈3-fold at $f_V = 0.23$ (a

linear increase was observed up to f_V = 0.23, followed by a sharp decline) in an earlier study [71]. Furthermore, another study found that dodecane reduced the k_La in a f_V-independent manner, while dispersed hexadecane offered enhancements to the k_La as f_V changed [103]. The results of the latter study are particularly confusing given that for both HCs $S_{VW} < 0$, - $S_{VW,hexadecane}$ is 3.6-fold lower than $S_{VW,dodecane}$, and that dispersed beading HCs typically provide a reduction or no changes in the k_La [14]. For spreading HCs, the k_La initially decreases quickly for low f_V and then gradually approaches the baseline value (i.e., that observed without the vector) [91, 102, 104].

2.5.5 Application to bacterial cultivation

Oxygen vectors have been applied widely and successfully to bacterial cultivations for the production of biopolymers, recombinant proteins and antibiotics. HA titer and MW were increased by ≈50% and 200%, respectively in *S. zooepidemicus* cultures in which 0.5% (v/v) hexadecane was added at the time of inoculation [11]. In the same study, the usage of dodecane (1% (v/v)) led to increased biomass relative to the cultivation with hexadecane, but negligible improvements to titer, although MW was increased by 100%. In an earlier study, the use of a PFC (perfluorodecalin) in *S. zooepidemicus* resulted in a 32% improvement in HA titer, although MW was not assessed [22]. Titers were slightly higher when using dispersed perfluorodecalin compared to a three-phase agitation strategy in which the agitation speed in a STR was increased from 200 to 600 rpm, although it is likely that the MW was substantially enhanced due to reduced shear stress. Dispersed heptane (0.3% v/v) provided ≈25% increases to titer and MW of poly(γ-glutamic acid) (PGA) produced in *B. subtilis* [23]. In the same study, the utilize of dodecane as vector decreased PGA titer and MW substantially, and the remarkable

difference in culture performance was attributed to a low NADH/NAD+ ratio and ATP levels when dodecane was applied. The application of hexane (1% (v/v)) and dodecane (0.5% (v/v)) as oxygen vectors resulted in respective 12% and 27% increases in the titer of ε-poly-lysine produced in cultures of *Streptomyces albulus*, while, surprisingly, oleic acid as dispersed phase (0.2% (v/v)) provided only a 7% increase in titer with hexane and oleic acid being spreading vectors and dodecane being beads [24]. Finally, the actinorhodin (antibiotic and pigment) titer doubled in cultures of *Streptomyces coelicolor* when using 10% (v/v) dispersed perfluorodecalin, while biomass was reduced proportionally [72]. The increase in culture performance resulted from the considerable improvements to the OUR and k_La (3 to 4-fold for both) due to the addition of vectors.

Chapter 3- Application of hydrocarbon and perfluorocarbon oxygen vectors to enhance heterologous production of hyaluronic acid in engineered *Bacillus subtilis*

Authors: Adam Westbrook[a], Xiang Ren[a], Murray Moo-Young[a], C. Perry Chou[a,*]

The research presented in this chapter was submitted for publication to the Biotechnology and Bioengineering Journal. Declaration: I initiated and conducted all experiments presented herein under the supervision of Dr. C. P. Chou and Dr. M. Moo-Young.

[a] Department of Chemical Engineering, University of Waterloo,
Waterloo, Ontario, Canada N2L 3G1

*Corresponding author: C. Perry Chou, Department of Chemical Engineering,
Adam Westbrook, Department of Chemical Engineering,
University of Waterloo, 200 University Avenue West, Waterloo, Ontario, Canada N2L 3G1

3.1 Introduction

Hyaluronic acid (HA) is a linear, unbranched polysaccharide consisting of alternating *N*-acetyl-D-glucosamine (GlcNAc) and D-glucuronic acid (GlcUA) monomers [1], and is used in the food, cosmetics, biomedical, and pharmaceutical industries [2]. At present, the US market for HA is estimated at over $1 billion annually, and is expected to rapidly increase with the demand for viscosupplements and dermal fillers [3]. Recently, HA production has shifted from direct extraction from animal and avian sources to microbial platforms in an effort to reduce production costs, increase supply, and avoid the risk of cross-species viral infection [105, 106]. Using attenuated strains of group C streptococci (i.e. *Streptococcus equisimilis* and *Streptococcus zooepidemicus*) is currently the dominant method of industrial HA production [3]. However, HA produced in streptococcal cultivations may contain endogenous exotoxins [2], and the fastidious nature of these organisms can increase manufacturing costs [107]. Accordingly, alternate microbial HA production hosts have received increasing attention in recent years [3]. In particular, *Bacillus subtilis* is a model Gram-positive bacterium amenable to genetic manipulation, grows well in inexpensive medium, has been granted a 'Generally Recognized as Safe (GRAS)' designation by the Food and Drug Administration, USA, and, therefore, has been applied to high-level and large-scale production of HA [3, 108].

Industrial bioprocesses based on microbial platforms are typically aerobic and utilize aqueous growth medium containing salts and other nutrients [27]. Oxygen is sparingly soluble in aqueous solutions, a limitation that is exacerbated by factors such as salinity and culture viscosity [6]. High-cell-density cultures are highly viscous, and, therefore, the diffusivity of oxygen becomes limited, causing a steep decline in dissolved oxygen (DO) levels [27, 109].

The increase in culture viscosity is more severe in bioprocesses in which high molecular weight (MW) biopolymers are secreted into the extracellular environment. For example, a substantial increase in viscosity (up to 500-fold) is observed as HA titers exceed 5 g/L in microbial cultivations [2]. Similarly, the production of xantham gum, a food additive and emulsifier, by *Xanthomonas campestris* can increase the culture viscosity by more than 100-fold [110]. The DO concentration is an intrinsic factor influencing HA synthesis due to a high demand of ATP for HA-producing cells [2, 10]. Oxygen transfer in microbial cultivations can be improved by increasing agitation and aeration rates, and, if necessary, pure oxygen supplementation. However, shearing due to high agitation and aeration rates may reduce the quality (i.e. MW) of HA [11, 68, 111], and supplementing pure oxygen can be detrimental to microorganisms as exposure to reactive oxygen species such as H_2O_2, O_2^-, and OH• can result in DNA instability, and protein and lipid denaturation [21]. Moreover, recombinant protein expression may be hampered by excessive DO levels due to misfolding, loss of activity, and protease degradation [112, 113]. Consequently, alternate methods to improve oxygen transfer in microbial cultivations for HA production are of significant interest, and using oxygen vectors is one of them.

Oxygen vectors are water-immiscible compounds possessing a greater capacity to dissolve oxygen compared to water. Hydrocarbons [19, 68-70], perfluorocarbons [22, 72, 89], vegetable oil [73], and silicone oil [17, 19] can enhance oxygen transfer in microbial cultivations, while insoluble polymers such as silicone rubber [19, 74], nylon [74], glass beads [74], Hytrel [19], Kraton [19], Desmopan [17, 19], and Elvax [17] have also been investigated as oxygen vectors. Oxygen vectors can enhance oxygen transfer by 1) creating large local

concentration gradients in the bulk aqueous phase by shuttling oxygen-rich vector droplets from the gas-liquid interface to the bulk liquid; 2) reducing surface tension at the air-water interface, resulting in reduced bubble coalescence and, in turn, smaller bubble diameter and increased interfacial area for oxygen transfer; and 3) colliding with and breaking air bubbles, in turn, reducing bubble diameter [17, 18]. Oxygen vectors are categorized based on their propensity to form discrete droplets (i.e. non-spreading) or films which spread over gas bubbles (i.e. spreading) in an aqueous phase, and the means by which they affect oxygen transfer may be dictated by their tendency to spread or lack thereof [14]. The selection of an appropriate oxygen vector can potentially reduce operating costs associated with power consumption from high agitation rates, compressed air delivery, and supplemental oxygen, and can reduce oxidative damage to the producing cell and target metabolite or protein, while also minimizing foaming during high-cell-density cultivations [19-21].

The application of hydrocarbon and perfluorocarbon oxygen vectors to microbial cultivations for HA production has been investigated, albeit to a limited extent. The addition of *n*-dodecane [114] and *n*-hexadecane [11] to *S. zooepidemicus* cultivations resulted in improvements to both the HA titer and MW, while perfluorodecalin also increased the HA titer in *S. zooepidemicus* cultivations relative to a three-stage agitation operation in which the agitation speed was increased in a step-wise manner [22]. However, these studies investigated only a few compounds as potential oxygen vectors, and no data is currently available on the application of oxygen vectors to heterologous HA production in common microbial hosts. In this study, we evaluated three hydrocarbons (i.e. *n*-heptane, *n*-hexadecane, and 2,2,4-trimethylpentane) and four perfluorocarbons (i.e. *n*-perfluorooctane, perfluorodecalin,

perfluoromethyldecalin, and perfluoro-1,3-dimethylcyclohexane) as potential oxygen vectors to enhance heterologous HA production in an engineered strain of *B. subtilis* with a significantly higher HA producing capacity than our previously reported strain [115]. Significant improvements to the HA titer and/or cell density were observed in cultures containing *n*-heptane, *n*-hexadecane, perfluoromethyldecalin, and perfluoro-1,3-dimethylcyclohexane, although the MW was marginally affected. We then manipulated the vector concentration and timing of addition, resulting in further improvements to the culture performance. Assessment of oxygen transfer via measuring the overall oxygen mass transfer coefficient k_La revealed that, regardless of spreading characteristics, hydrocarbon vectors slightly reduced k_La over the low vector concentrations employed in this study, while perfluoromethyldecalin enhanced oxygen transfer. We also investigated culture performance at higher agitation rates, and observed that the addition of *n*-hexadecane or perfluoromethyldecalin further enhanced the HA titer and cell density, although the MW was somewhat reduced when *n*-hexadecane was present, suggesting that functional expression of hyaluronan synthase (HAS) may be affected by *n*-hexadecane exposure in *B. subtilis*. Moreover, our results indicate that higher shear rates may somehow drive more carbon flux through the HA biosynthetic pathway without negatively affecting the MW.

3.2 Materials and Methods

Bacterial strains and plasmid construction: *Escherichia coli* HI-Control™ 10G chemically competent cells (Lucigen; Wisconsin, USA) were prepared as electrocompetent cells as described previously [116] and used as host for plasmid construction. Strain 1A751 is a derivative of *B. subtilis* 168 (i.e. *B. subtilis* 168 *his npr*R2 *npr*E18 Δ*aprA*3 Δ*eglS*102 Δ*bglT*

*bglS*RV) that has proven to be an effective host for heterologous HA production [115, 117, 118]. *B. subtilis* and *E. coli* strains were maintained as glycerol stocks at -80 °C. To construct the genomic integration vector pAW009, promoter $P_{grac.UPmod}$ was amplified from pHT01 [119] with primers Pgrac.UPmod,SalI.f (5'-cagattgagtcgac**ggatcactag**aaaatttttatcttatcacttgaaattgg-3') and Pgrac.UPmod.BamHI.r (5'-gcacttgaggatcctcctcctttaattggg-3'), followed by insertion into SalI/BamHI-digested pAW008 [117] as shown in Figure 9 (restriction sites are underlined in the primer sequences). $P_{grac.UPmod}$ (i.e. promoter P61) is a weaker derivative of promoter P_{grac} (i.e. promoter P01) that contains a modified upstream promoter element (UP) that reduces the relative promoter strength by approximately half [120] [Note that the modified UP was introduced with primer Pgrac.UPmod,SalI.f and the modified sequence is in bold font.]. Transformation of pAW009 into *B. subtilis* results in the integration of a $P_{grac.UPmod}$::*seHas*:*tuaD* expression cassette at the *amyE* locus as shown in Figure 9 [*tuaD* encodes native uridine diphosphate (UDP)-glucose-6 dehydrogenase (TuaD) and *seHas* encodes hyaluronan synthase from *S. zooepidemicus* (SeHAS)]. Competent cell preparation and transformation of pAW009 was performed as previously described [117].

Cultivation medium and conditions: *B. subtilis* strains were plated on non-select LB agar (NaCl, 5 g/L; yeast extract, 5 g/L; tryptone, 10 g/L; agar, 15 g/L), and grown overnight at 37 °C. Shake flask cultures to compare HA production in AW008 and AW009 were performed as previously described [115]. To prepare the seed cultures for bioreactor cultivations, a single colony was used to inoculate 25 mL prewarmed non-select LB, and grown for ~8 h at 37 °C and 280 revolutions per minute (rpm) to generate the starter culture. The starter culture was

subsequently diluted 100-fold into 100 mL prewarmed non-select LB, and grown for ~13 h at 37 °C and 280 rpm to generate the seed culture. Cultivations were performed in a New Brunswick™ BioFlo® 115 bioreactor (Hamburg, Germany) under the following conditions: 0.7 L working volume (1.3 L vessel), 2 volume per volume per minute (vvm) [i.e. 1.4 L/min] air, 300 rpm, 37 °C, pH 7 (3 M NH_4OH). The non-select cultivation medium was of the following composition (per L): sucrose, 30 g; $(NH_4)_2SO_4$, 1 g; $K_2HPO_4 \cdot 3H_2O$, 9.15 g; KH_2PO_4, 3 g; trisodium citrate· $2H_2O$, 1 g; yeast extract, 10 g; $CaCl_2$, 5.5 mg; $FeCl_2 \cdot 6H_2O$, 13.5 mg; $MnCl_2 \cdot 4H_2O$, 1 mg; $ZnCl_2$, 1.7 mg; $CuCl_2 \cdot 2H_2O$, 0.43 mg; $CoCl_2 \cdot 6H_2O$, 0.6 mg; $Na_2MoO_4 \cdot 2H_2O$, 0.6 mg. The bioreactor was inoculated with 10% volume per volume (v/v) of the seed culture.

Determination of k_La: Experiments to determine k_La were performed under the same cultivation conditions described above without the inoculum. Measurements of k_La were performed using the dynamic "gas out-gas in" method, and the probe response time was neglected due to the relatively low k_La values obtained under our experimental conditions [34]. k_La values were obtained from the mass balance equation:

$$ln\left(\frac{DO^* - DO(t)}{DO^* - DO(t_0)}\right) = -k_L a(t - t_0) \quad (10)$$

where DO^* is the saturation reading of the probe.

Oxygen vectors: *n*-heptane (>99%), *n*-hexadecane (>99%), *n*-perfluorooctane (98%), perfluorodecalin (95%), and perfluoro-1,3-dimethylcyclohexane (80%) were obtained from MilliporeSigma (MO). Perfluoromethyldecalin (80%), a mixture of perfluoro-1-methyldecalin and perfluoro-2-methyldecalin, was also obtained from MilliporeSigma. *n*-Heptane (>99%)

was obtained from J.T. Baker (NJ). The physical properties of oxygen vectors used in this study are summarized in Table 1.

HA purification and analysis: Cultivation samples were diluted appropriately in phosphate buffered saline (NaCl, 8 g/L; KCl, 0.2 g/L; Na_2HPO_4, 1.44 g/L; KH_2PO_4, 0.24 g/L), and HA was purified with cetylpyridinium chloride as previously described [118]. HA titer was determined using the modified carbazole assay [121], and MW was analyzed via agarose gel electrophoresis [122] with slight modifications. 2 µg of purified HA was loaded per well, and gels stained O/N in 0.005% Stains-All (50% v/v ethanol) were destained for ~8 h in 20% v/v ethanol, followed by destaining for ~16 h in 10% v/v ethanol. Gels were then photobleached for 20 min on a LED light box, and scanned with an Epson Perfection V600 Photo scanner (Epson; Nagano, Japan). Scanned images were analyzed using ImageJ [123], and data analysis was performed as previously described [122]. Duplicate samples were analyzed.

3.3 Results

3.3.1 Derivation of an improved strain of B. subtilis for HA production

We previously constructed a strain of *B. subtilis* capable of high-level production of high MW HA, in which coexpression of *seHas* and *tuaD* was driven by the strong promoter P_{grac}, i.e. strain AW008 [115]. Note that coexpression of hyaluronan synthase (e.g. SeHAS) and UDP-glucose-6 dehydrogenase (e.g. TuaD) is required for high-level HA production in *B. subtilis* [2]. In the same study, we observed that reducing the strength of the promoter driving cardiolipin overproduction in a derivative of AW008 in which the membrane cardiolipin content had been artificially enhanced, improved the HA titer by 30%, with a relatively small reduction in the MW. This prompted us to examine the effects of *seHas* and *tuaD* expression

on HA production via construction of strain AW009, in which the coexpression of both genes was driven by promoter $P_{grac.UPmod}$, i.e. a derivative of P_{grac} for which the relative promoter strength is ~0.5 [120]. AW009 was constructed via transformation of 1A751 with NdeI-linearized pAW009 (Figure 9). Similar to AW008, AW009 presented a mucoid phenotype characteristic of HA-producing strains of *B. subtilis* [2], and was genetically stable based on the persistence of the mucoid phenotype upon revival. AW009 produced approximately twice as much HA as AW008 (i.e. 0.97 g/L for AW009 compared to 0.48 g/L for AW008; Figure 10A) after 10 h in shake flask cultures, while the MW declined by only 12% (Figure 10B). Moreover, the cell density in cultures of AW009 after 10 h was OD_{600} 6.1, representing a 45% increase compared to that of AW008 (Figure 10C). The improved growth of AW009, compared to AW008, may have contributed to the improved HA titer in cultures of AW009 as HA is a growth-associated product [10], although it is unclear as to why AW009 reached a higher cell density. UDP-GlcNAc is the limiting substrate for HA biosynthesis in *S. zooepidemicus*, such that expression of *hasD*, encoding UDP-GlcNAc pyrophosphorylase (HasD), and/or *hasE*, encoding glucose-6-P isomerase (HasE), improved the MW of HA, relative to the wild-type strain [124] [Note that both HasD and HasE are involved in UDP-GlcNAc synthesis in *S. zooepidemicus*.]. Accordingly, the slight reduction in MW in cultures of AW009, compared to AW008, may have resulted from the reduced expression of *tuaD*, which should reduce the ratio of UDP-GlcUA (i.e. the limiting substrate for HA production in *B. subtilis*) to UDP-GlcNAc. Based on the overall performance of AW009, compared to AW008, it was selected as the host for HA production in our assessment of various oxygen vectors.

Genomic integration vector pAW009 was constructed by amplifying promoter $P_{grac.UPmod}$ from pHT01, followed by insertion into SalI/BamHI-digested pAW008. $P_{grac.UPmod}$ is a weaker derivative of promoter P_{grac} that has a modified upstream promoter element (UP) that reduces the relative promoter strength by approximately half. AW009 was constructed via transformation by natural competence of 1A751 with NdeI-linearized pAW009, resulting in the integration of a $P_{grac.UPmod}$::*seHas*:*tuaD* expression cassette and neomycin resistance marker (i.e. *npt*, encoding neomycin phosphotransferase) at the *amyE* locus. AW009 constitutively expresses *seHas* and *tuaD*, respectively encoding hyaluronan synthase from *S. zooepidemicus* (SeHAS) and native UDP-glucose-6 dehydrogenase (TuaD), resulting in the production of high MW HA and, in turn, encapsulation of AW009. AW009 produced approximately twice as much HA as our previous production strain, i.e. AW008, which was constructed via transformation of 1A751 with NdeI-linearized pAW008. Other genes and abbreviations: *bla* encodes β-lactamase for selection of *E. coli* on ampicillin; *amyE* encodes native α-amylase; origin of replication (ori); genomic DNA (gDNA).

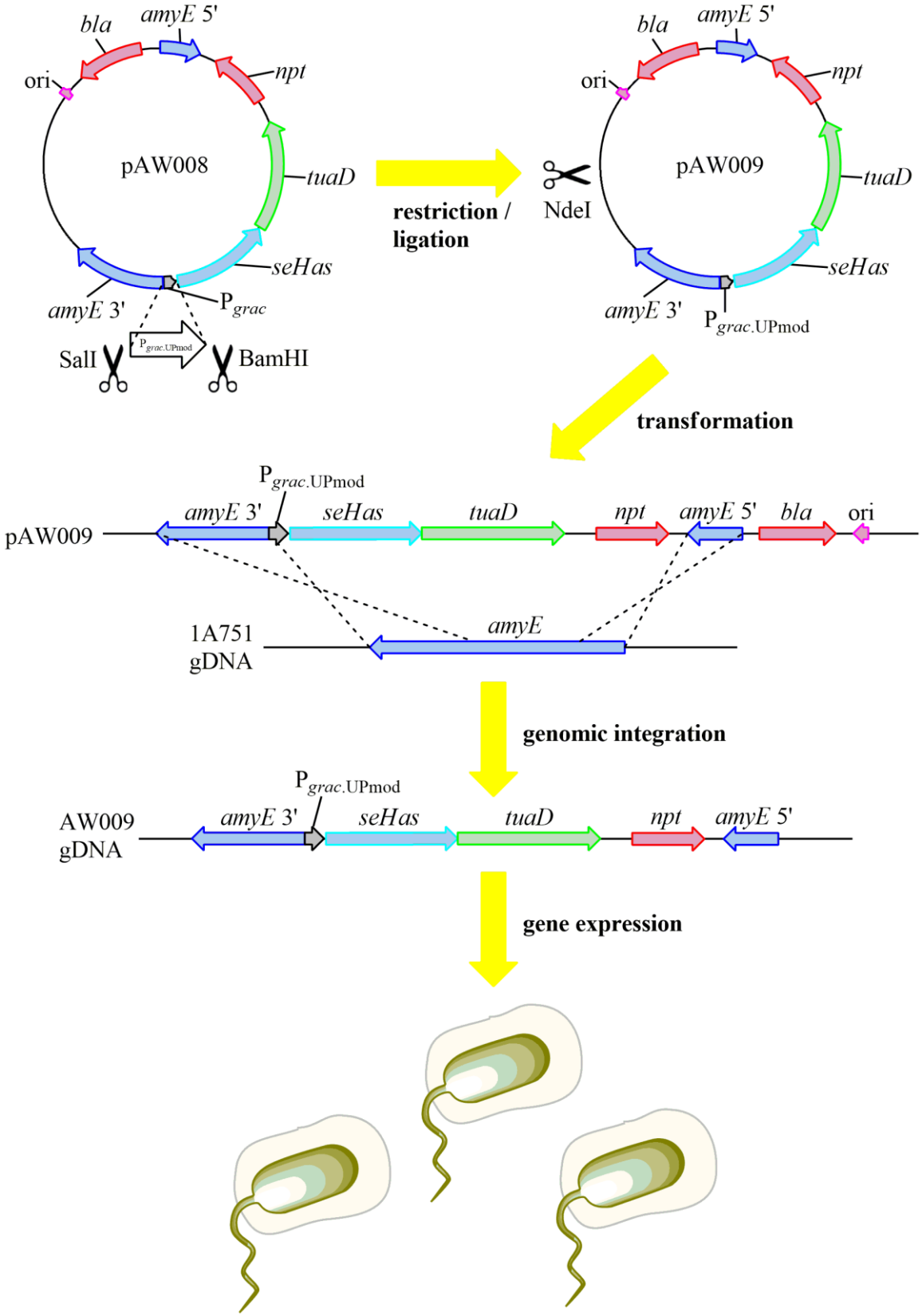

Figure 9: The derivation of an improved strain of B. subtilis for heterologous HA production.

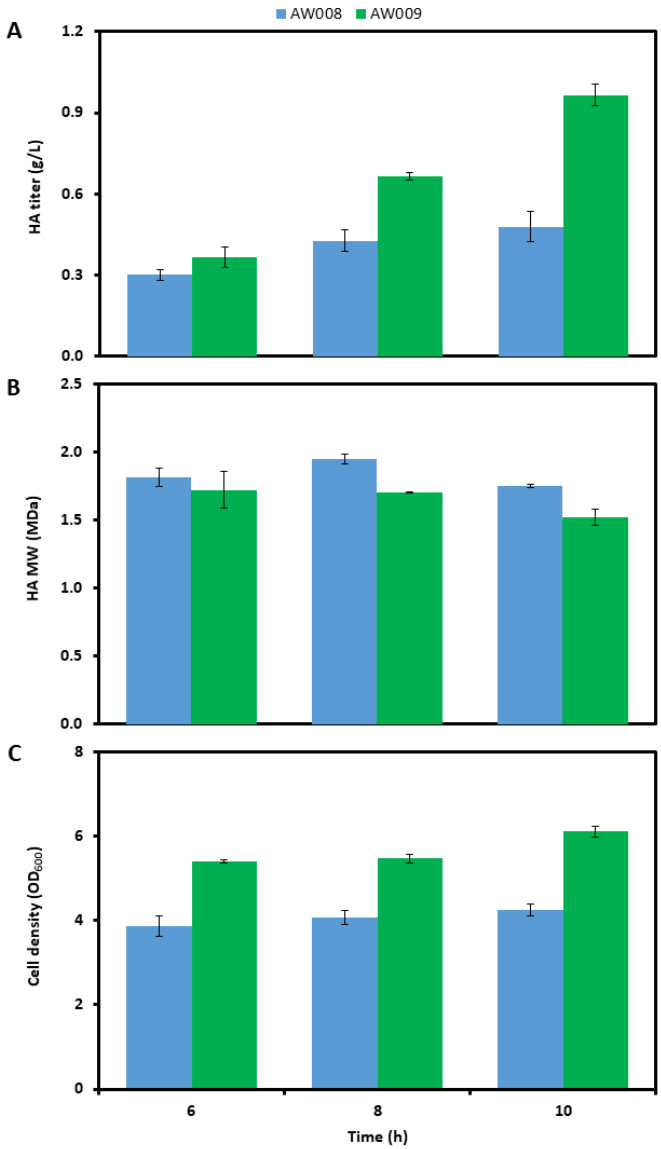

Figure 10: Time profiles of A) HA titer, B) HA MW, and C) cell density in shake flask cultures of AW008 and AW009. SD of experiments performed in triplicate are shown in Panels A and B, and SD of duplicate samples are shown in Panel C.

3.3.2 Preliminary evaluation of potential oxygen vectors

Three hydrocarbons and four perfluorocarbons were evaluated for their effects on HA production in batch cultivations of strain AW009 in a bench-scale stirred-tank reactor (STR). Potential oxygen vectors were selected based on their volatility (i.e. a minimum normal boiling point of ~100 °C) and relative oxygen solubility (i.e. at least 8-fold higher than water).

Compounds such as *n*-heptane, *n*-hexadecane, and perfluorodecalin were preferred as they had been successfully applied to either microbial HA production [11, 22] or biopolymer production in *B. subtilis* [23]. In the preliminary evaluation, each compound was added to the cultivation medium at a concentration of 1% v/v 2 h after inoculation. A relatively low agitation rate at 300 rpm was used to minimize potential HA degradation resulting from polymer shearing [68].

Compound	**Molecular formula / structure**	**Dynamic viscosity (mPa·s)**	**Density (g/mL)**	**Boiling point (°C)**	**Relative oxygen solubility***	**References**
n-hexadecane	$C_{16}H_{34}$ (linear)	3.0	0.77	287	8.2	[125, 126]
n-heptane	C_7H_{16} (linear)	0.39	0.68	98.4	10.8	[127, 128]
2,2,4-trimethylpentane	C_8H_{18} (branched)	3.19	0.77	99	14.0	[129, 130]
perfluoro-1,3-dimethylcyclohexane	C_8F_{16} (cyclic, branched)	1.92	1.83	102	16.1[a]	[131, 132]
perfluoromethyldecalin	$C_{11}F_{20}$ (bicyclic, branched)	6.47	1.95	137-160	12.7	[133, 134]
perfluorodecalin	$C_{10}F_{18}$ (bicyclic)	5.41	1.91	142	13.9[b]	[131, 135]
n-perfluorooctane	C_8F_{18} (linear)	1.26	1.77	103	14.0[c]	[135, 136]

*Expressed as the fold increase in oxygen solubility relative to water. Measured at 16 °C[a], 38 °C[b], and 36 °C[c]

Table 1: Physical properties of oxygen vectors used in this study measured at 25 °C and atmospheric pressure unless otherwise indicated.

AW009 produced 992 mg/L of HA after 12 h (Figure 11A) with a peak MW of 1.2 MDa at 8 h, (Figure 11B), and final cell density of OD_{600} 12.8 (Figure 11C). The DO fell below 5% saturation after 4 h where it remained for the rest of the cultivation (Figure 11D). The addition of *n*-hexadecane resulted in a 34% increase to the final HA titer (1327 mg/L; Figure 11A), although the MW was not significantly affected (Figure 11B). Moreover, the cell growth rate was improved such that the final cell density (OD_{600} 13.3) was obtained at 10 h, compared to 12 h without the vector (Figure 11C). Notably, *n*-hexadecane was the only compound tested that provided a substantial increase in DO levels, which remained above 10% saturation throughout the cultivation (Figure 11D). While the addition of *n*-heptane did not markedly affect the volumetric HA titer, it did improve the specific HA titer by 26%, i.e. 97.6 mg/(L·OD_{600}) for *n*-heptane compared to 77.5 mg/(L·OD_{600}) with no vector. Moreover, the addition of *n*-heptane prolonged the oxygen limitation by 1 h compared to the cultivation without the vector (Figure 11D).

Two of the four perfluorocarbons tested, i.e. perfluoro-1,3-dimethylcyclohexane and perfluoromethyldecalin, significantly improved culture performance. The addition of perfluoro-1,3-dimethylcyclohexane and perfluoromethyldecalin resulted in 50% (1490 mg/L) and 49% (1481 mg/L) increases to the final HA titer (Figure 11A), respectively, although the MW was not significantly affected (Figure 11B). Moreover, the respective final cell densities increased by 16% (OD_{600} 14.8) and 11% (OD_{600} 14.2) relative to the cultivation with no vector (Figure 11C) although DO levels were marginally improved (Figure 11D). Conversely, the addition of *n*-perfluorooctane resulted in a 23% decrease to the HA titer (761 mg/L; Figure 11A), and an 11% decrease in the final cell density (OD_{600} 11.4; Figure 11C). The specific HA

titer was highest for the cultivation with perfluoromethyldecalin (104.7 mg/(L·OD_{600})), compared to all other vectors, and was 35% higher relative to the cultivation with no vector.

For initial experiments with *n*-hexadecane and perfluoro-1,3-dimethylcyclohexane, the oxygen vectors were added at the time of seed culture inoculation. However, the addition of 2,2,4-trimethylpentane and perfluoromethyldecalin at the time of inoculation completely inhibited growth, such that in subsequent experiments all vectors were added 2 h after inoculation when the exponential growth phase was reached. This bioprocessing strategy was developed based on the prior observation that 2,2,4-trimethylpentane is toxic to *E. coli* in the stationary phase, but is not during exponential growth [137]. Adding *n*-hexadecane at the time of inoculation resulted in a 30% increase in the final HA titer (1731 mg/L; Figure 12A), a 14% increase in the final MW (1.14 MDa; Figure 12B), and a 22% increase in the final cell density (OD_{600} 16.1; Figure 12C), although DO levels were lower between 5 h and 8 h (Figure 12D), compared to the addition of *n*-hexadecane at 2 h. The addition of perfluoro-1,3-dimethylcyclohexane at the time of inoculation resulted in a small increase in the final HA titer (1576 mg/L; Figure 12A), although the titer after 10 h was similar to the final titer when the vector was added at 2 h (Figure 12A). In addition, the peak MW dropped from 1.34 MDa to 1.26 MDa, (Figure 12B), and the final cell density increased by 15% (OD_{600} 17; Figure 12C), although the DO profiles were not significantly different (Figure 12D).

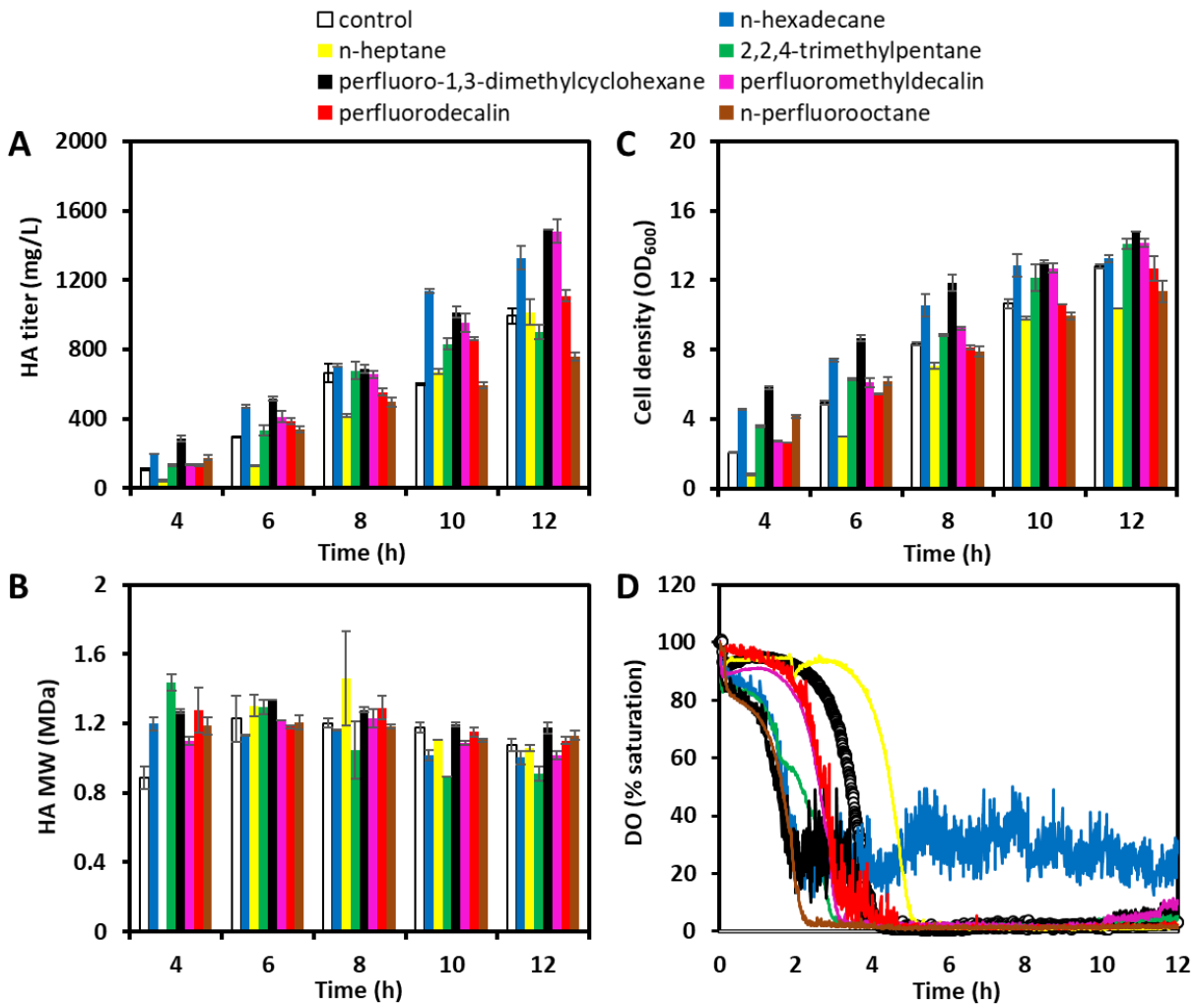

Figure 11: Time profiles of A) HA titer, B) HA MW, C) cell density, and D) DO in cultures of AW009 with no vector, or other seven selected vectors.

Selected vectors include *n*-hexadecane, *n*-heptane, 2,2,4-trimethylpentane, perfluoro-1,3-dimethylcyclohexane, perfluoromethyldecalin, perfluorodecalin, or *n*-perfluorooctane which was added 2 h after inoculation at a final concentration of 1% v/v. SD of duplicate samples shown in Panels A, B, and C.

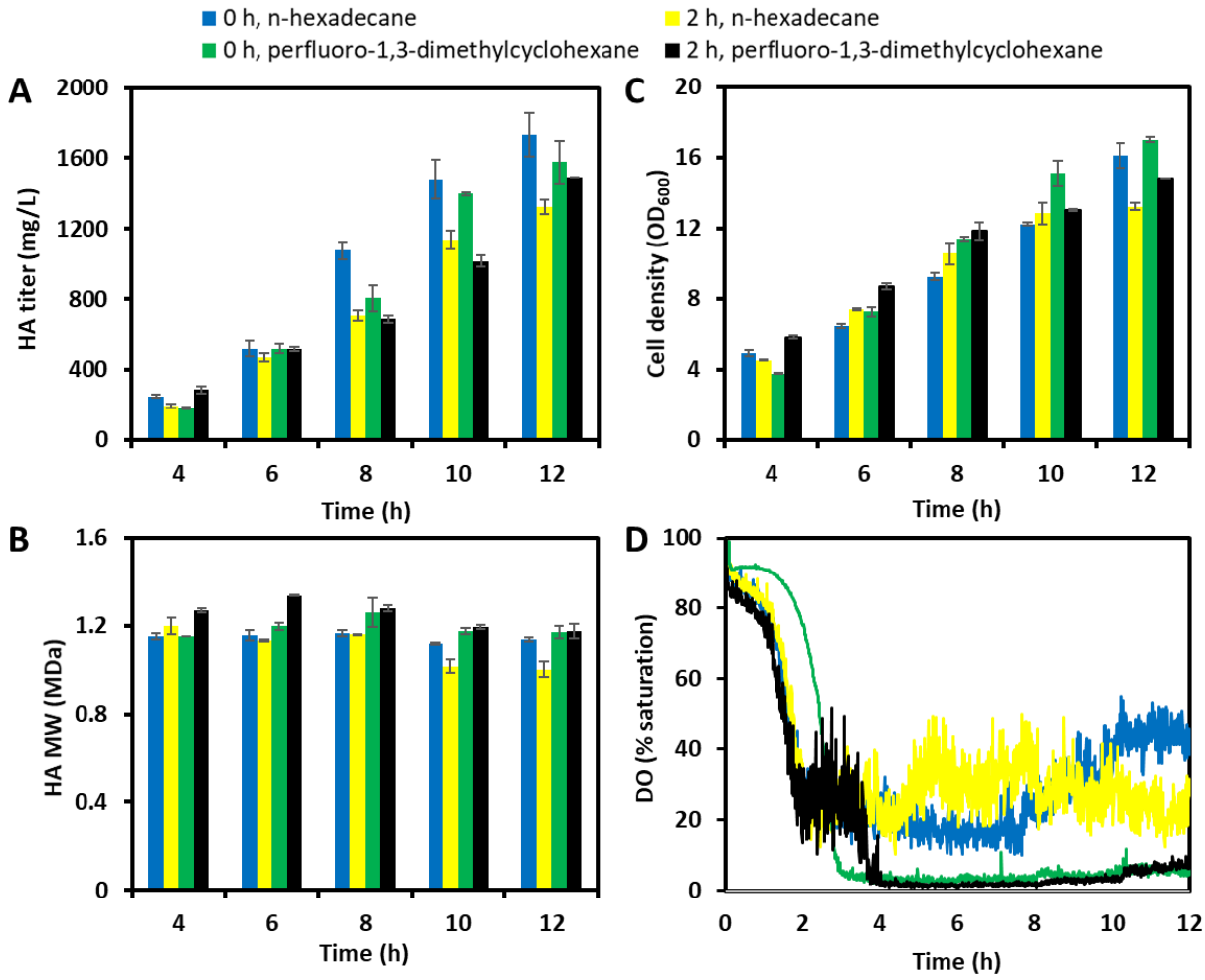

Figure 12: Time profiles of A) HA titer, B) HA MW, C) cell density, and D) DO in cultures of AW009 in which n-hexadecane or perfluoro-1,3-dimethylcyclohexane was added at the time of inoculation (0 h) or 2 h after inoculation at a final concentration of 1% v/v. SD of duplicate samples shown in Panels A, B, and C.

3.3.3 Vector concentration affects HA production

Based on the results from the preliminary evaluation, *n*-hexadecane provided the greatest enhancements to DO levels and HA production. Accordingly, we attempted to further improve culture performance by manipulating the *n*-hexadecane concentration. Reducing the *n*-hexadecane concentration to 0.5% v/v increased the final HA titer by 20% (1596 mg/L; Figure 13A), without significantly affecting the MW (Figure 13B). The final cell density also

increased by 22% (OD_{600} 17.4; Figure 13C), which may be attributed, in part, to the increase in DO levels after 6 h (Figure 13D). Our results are similar to an earlier report of enhanced HA production in batch cultures of *S. zooepidemicus* upon the addition of *n*-hexadecane to 0.5% v/v, which maximized k_La [11]. In contrast, adding *n*-hexadecane to 1% v/v was found to be optimal for poly(γ-glutamic acid) [PGA] production in *B. subtilis* [23]. The application of *n*-heptane as an oxygen vector to enhance PGA production in cultures of *B. subtilis* resulted in greater improvements to both the titer and MW, compared to cultures supplemented with *n*-hexadecane, and the optimal concentration of *n*-heptane (0.3% v/v) was significantly lower compared to *n*-hexadecane (1% v/v) [23]. On the other hand, we obtained significantly higher HA titers with *n*-hexadecane compared to *n*-heptane (Figure 3A), albeit with a slight reduction in MW (Figure 3B). Given that our preliminary evaluation was conducted with a vector concentration of 1% v/v, we considered that reducing the *n*-heptane concentration might improve culture performance. Reducing the *n*-heptane concentration to 0.4% v/v resulted in a 20% increase in the final HA titer (1192 mg/L; Figure 14A), and the titer after 10 h reached 1123 mg/L, compared to only 672 mg/L for the cultivation containing 1% v/v *n*-heptane (Figure 14A). However, the MW was not improved by reducing the *n*-heptane concentration (Figure 14B). The increase in the final titer was proportional to the increase in the final cell density (OD_{600} 12.7; Figure 14C), which is plausible considering that HA is a growth-associated product [10]. The DO levels declined quickly prior to the addition of 0.2% *n*-heptane, compared to the cultivation with no vector, and were only temporarily rescued upon adding *n*-heptane, before dropping to approximately 0% saturation at around 3 h (Figure 14D). Similarly, the addition of 0.4% v/v *n*-heptane did not delay oxygen limitation, compared to the cultivation

with no vector, such that in both cultivations the DO level fell below 5% saturation after approximately 4 h (Figure 14D). This is in contrast to the cultivation containing 1% v/v *n*-heptane in which oxygen limitation was postponed by approximately 1 h.

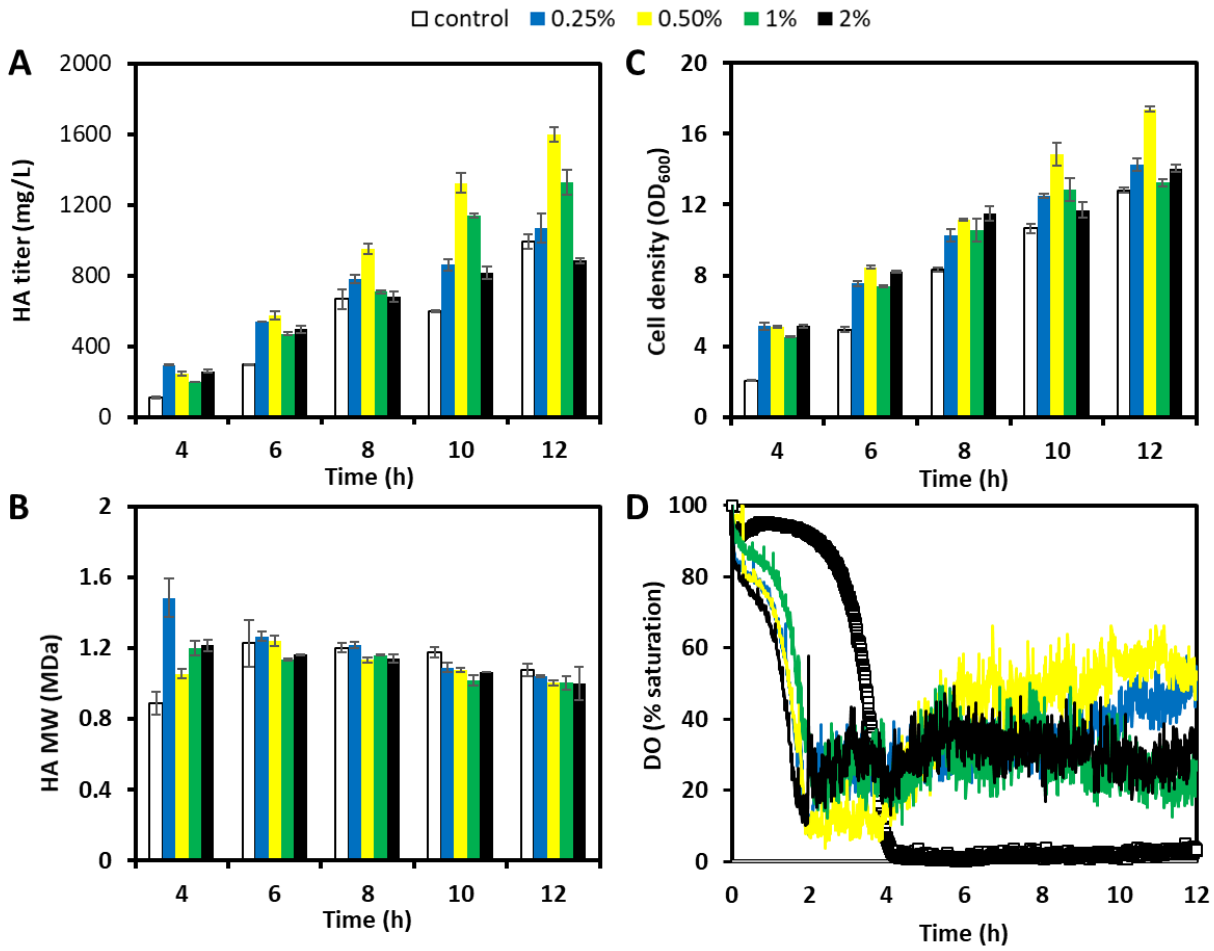

Figure 13: Time profiles of A) HA titer, B) HA MW, C) cell density, and D) DO in cultures of AW009 with no vector, or in which n-hexadecane was added 2 h after inoculation at a final concentration of 0.25%, 0.5%, 1%, or 2% v/v. SD of duplicate samples shown in Panels A, B, and C.

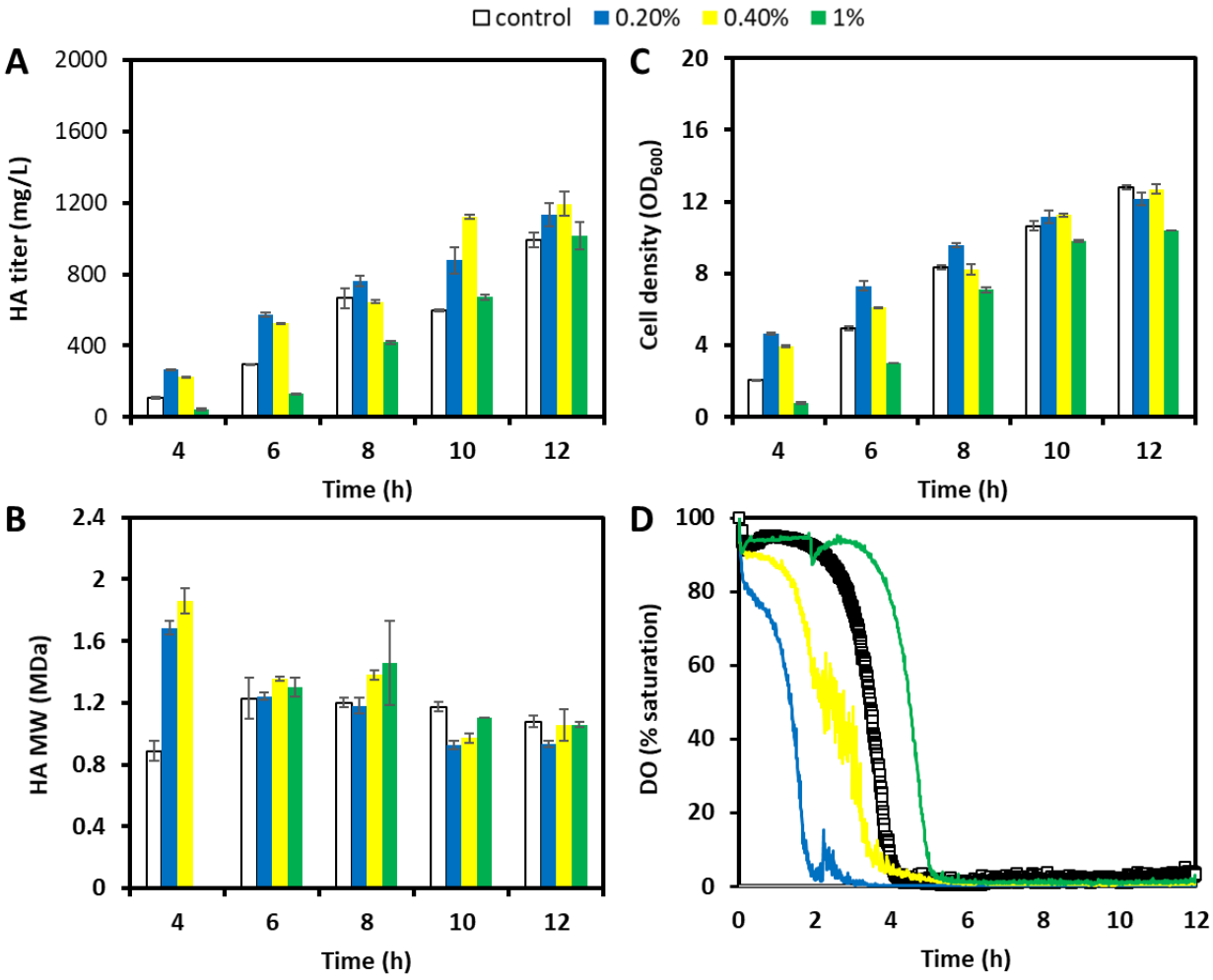

Figure 14: Time profiles of A) HA titer, B) HA MW, C) cell density, and D) DO in cultures of AW009 with no vector, or in which n-heptane was added 2 h after inoculation at a final concentration of 0.2%, 0.4%, or 1% v/v. SD of duplicate samples shown in Panels A, B, and C.

Due to the high specific HA titer observed in the cultivation containing perfluoromethyldecalin, and its lower cost compared to perfluoro-1,3-dimethylcyclohexane, we further evaluated the effect of perfluoromethyldecalin concentration on HA production. Reducing the perfluoromethyldecalin concentration to 0.5% v/v resulted in culture performance similar to the cultivation with no vector (Figures 15A-D). Moreover, further increasing the perfluoromethyldecalin concentration to 2% v/v slightly improved the final HA

titer (Figure 15A) and cell density (Figure 15C), although the MW (Figure 15B) and DO (Figure 15D) profiles were essentially unaffected, compared to 1% v/v. In spite of the delay in reaching oxygen limitation by 2 h upon adding perfluoromethyldecalin to 3% v/v, the final HA titer and cell density were not improved, compared to 2% v/v, and the MW declined potentially due to an increase in viscosity with increasing perfluoromethyldecalin concentration [138].

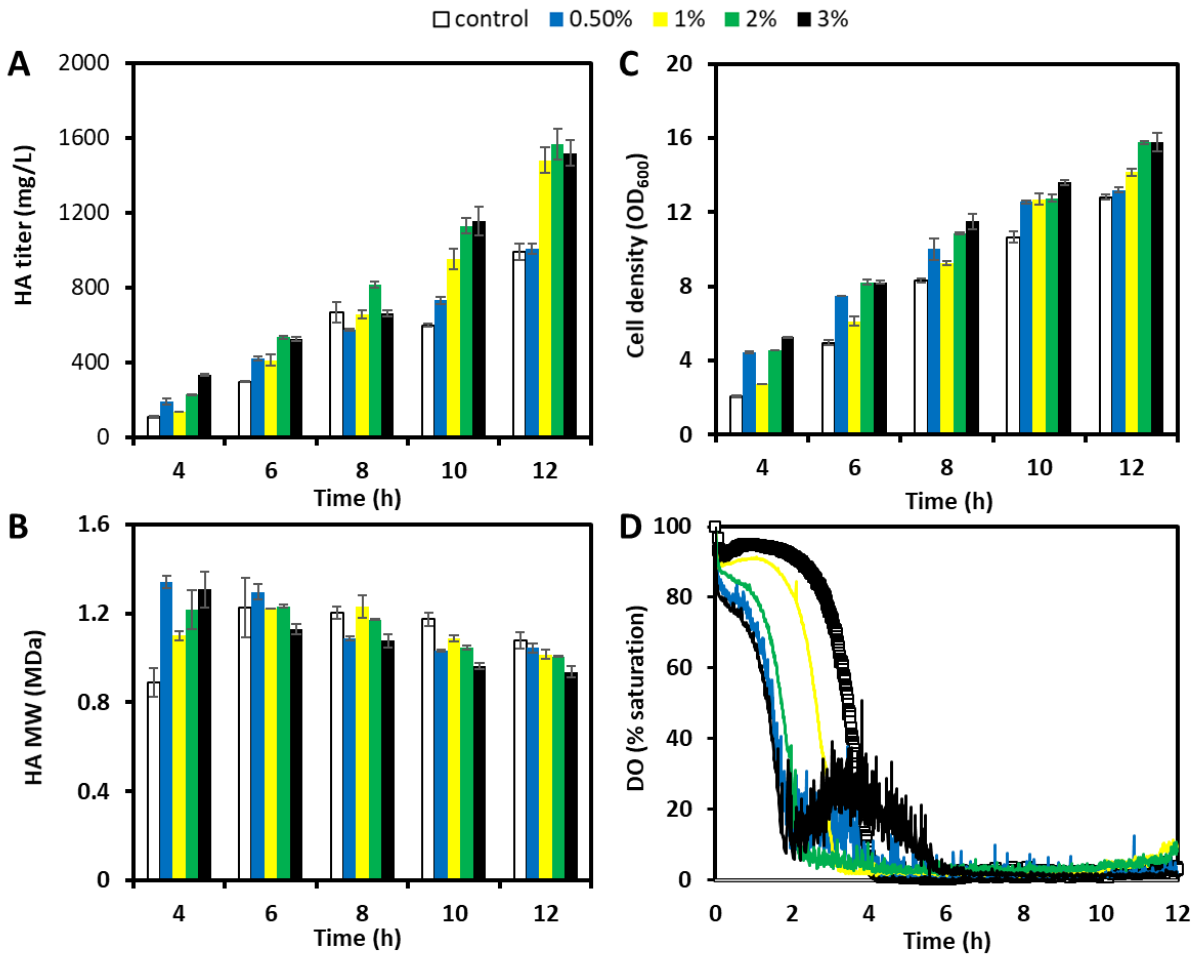

Figure 15: Time profiles of A) HA titer, B) HA MW, C) cell density, and D) DO in cultures of AW009 with no vector, or in which perfluoromethyldecalin was added 2 h after inoculation at a final concentration of 0.5%, 1%, 2%, or 3% v/v. SD of duplicate samples shown in Panels A, B, and C.

3.3.4 The effect of oxygen vectors on oxygen mass transfer

In an attempt to understand how oxygen vectors can enhance HA production in *B. subtilis*, we assessed oxygen mass transfer in our cultivation system. The addition of 0.25% v/v *n*-hexadecane resulted in a modest decrease in k_La, although increasing the concentration to 2% v/v had essentially no further effect on k_La (Figure 16A). The magnitude and trend of our k_La estimates with increasing *n*-hexadecane concentration are consistent with previous work in which k_La decreased modestly for concentrations up to 2.5% v/v during the operation at 288 rpm and 1 vvm air-purging [11]. In contrast to our results, an initial increase in k_La was observed at low *n*-hexadecane concentrations (i.e. < 2.5% v/v), followed by a decline in k_La at higher *n*-hexadecane concentrations until phase inversion occurred (i.e. the culture becomes a continuous phase when the vector concentration is high enough) [139]. However, the latter study employed surface aeration in a STR operated at 1000 rpm such that direct comparison of results is difficult. As was the case for *n*-hexadecane, the addition of *n*-heptane at 0.2% v/v resulted in a modest decrease to k_La, and increasing the concentration to 1% v/v did not appreciably affect k_La (Figure 16B). In contrast to our results, the addition of *n*-heptane at 0.1% v/v in a STR operated at 300 rpm and 0.5 vvm resulted in a 15% increase in k_La, and increasing the *n*-heptane concentration to 5% v/v increased k_La by 175% [140]. On the other hand, simultaneously increasing the agitation and aeration rates to 400 rpm and 1 vvm, respectively, resulted in an initial 50% reduction in k_La for *n*-heptane concentrations up to 1% v/v, followed by a gradual increase in k_La with a further increase in the *n*-heptane concentration [140]. Accordingly, the effect of *n*-heptane on k_La in aerated STRs appears to vary considerably with agitation and aeration rates, such that our observation of a slight reduction in k_La was considered reasonable. Finally, *n*-heptane can dramatically increase k_La in bubble column

reactors as both vector concentration and superficial gas velocity are increased [141]. In general, non-spreading hydrocarbons (e.g. *n*-hexadecane) negatively or hardly affect k_La [14], although at lower vector concentrations k_La may increase due to the shuttling effect, through which vector droplets briefly contact the air bubble surface and subsequently transfer oxygen to the bulk aqueous phase [19, 140]. Alternatively, spreading hydrocarbons (e.g. *n*-heptane) generally induce an initial decrease in k_La at low concentrations, followed by a gradual increase in k_La with increasing concentration [91, 102, 104, 140]. It was hypothesized that the initial decrease in k_La resulted from increased liquid phase resistance due to the accumulation of surface active contaminants at the gas-water interface, and that the gas bubble size decreased with an increasing vector concentration as the system approached phase inversion [91, 104]. An alternate/complementary explanation is that the vector film forming around air bubbles becomes unstable with increasing thickness as the vector concentration increases, resulting in the release of oxygen-rich droplets into the bulk aqueous phase [140].

While *n*-hexadecane and *n*-heptane slightly reduced k_La, perfluoromethyldecalin had the opposite effect such that k_La increased with increasing concentration up to 2% v/v, resulting in a maximum increase of 35% in k_La compared to the control with no vector (Figure 16C). While k_La measurements for perfluoromethyldecalin are not available in the literature, perfluorodecalin, a structurally similar vector, was observed to increase k_La in a STR at concentrations up to 20% v/v, using the same agitation rate and lower aeration (1.1 vvm) compared to our study, resulting in a maximum increase of ~70% in k_La [142]. Similarly, the addition of perfluorodecalin to 5% v/v provided a slight increase in k_La in a STR operated at 300 rpm and 0.5 vvm air-purging, while increasing the concentration to 10% v/v resulted in a

40% increase in k_La [143]. The addition of forane F66E, an unsaturated perfluorocarbon, to *Aerobacter aerogenes* cultures operated at 400 rpm and 0.21 vvm air-purging, increased k_La for concentrations up to 23% v/v, resulting in a maximum increase of ~250% in k_La [89]. Accordingly, a consensus seems to exist regarding the positive influence of perfluorocarbons on oxygen transfer in biological cultivation systems, and this is in line with our observations.

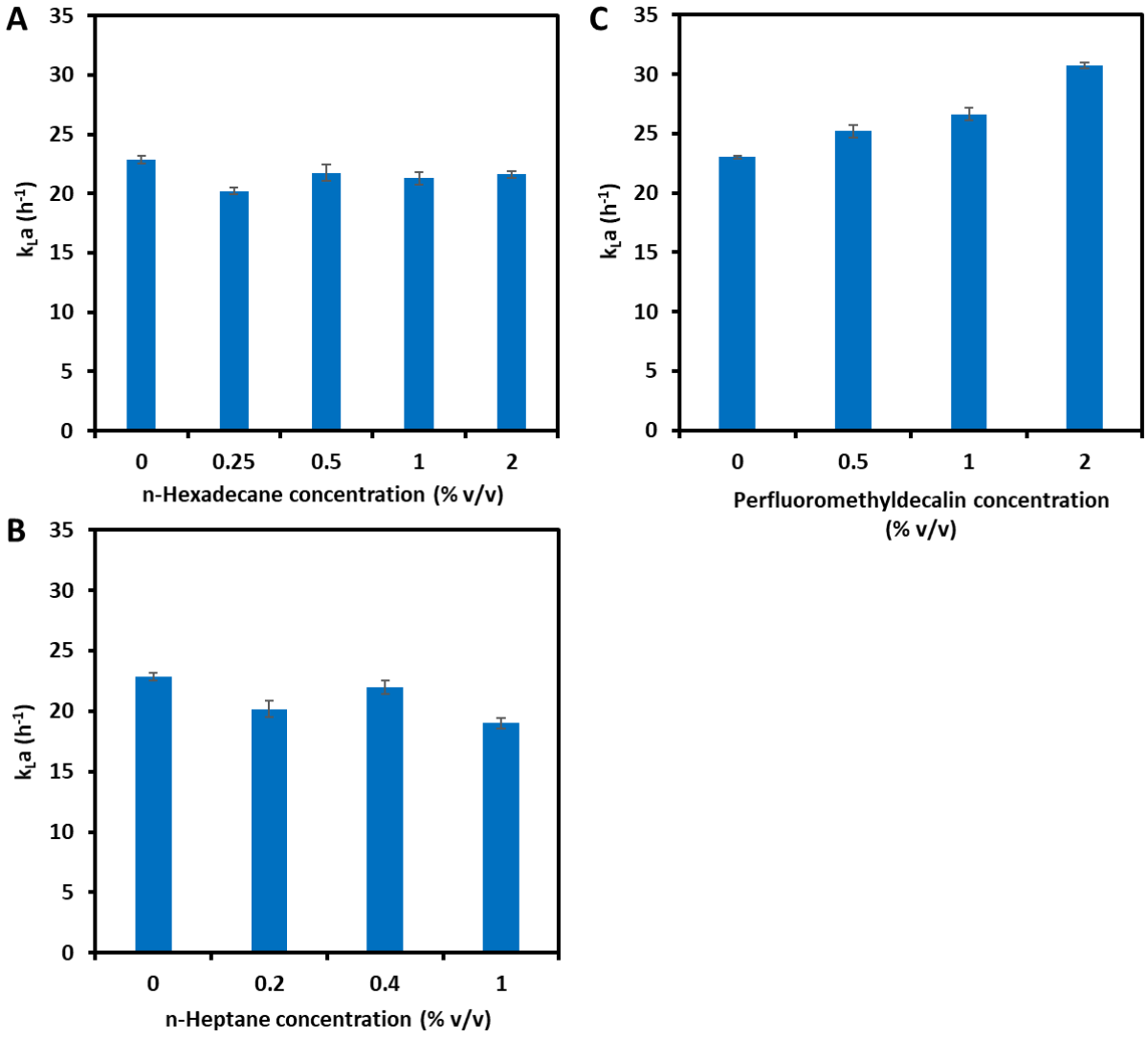

Figure 16: k_La determined for different concentrations of A) n-hexadecane, B) n-heptane, and C) perfluoromethyldecalin. Experimental conditions described in M&M. SD of three experiments shown.

3.4 Discussion

Simultaneously achieving a high MW and titer in cultivations for HA production is a challenging task. Generally, it requires a high carbon flux through both branches of the HA biosynthetic pathway to ensure a sufficient and balanced monomer supply of UDP-GlcNAc and UDP-GlcUA [124]. Moreover, an adequate supply of oxygen is essential to generate the substantial amount of ATP consumed during HA biosynthesis, and this is particularly challenging due to the rapid increase in culture viscosity with increasing HA titer [2, 22]. To further complicate matters, the functional expression of HAS to maximize HA production is dependent on its specific orientation with certain lipids in the cell membrane [115, 144]. Here we have shown that hydrocarbon and perfluorocarbon oxygen vectors can significantly increase the HA titer in *B. subtilis* cultures. However, certain vectors may reduce the efficacy with which streptococcal Class I HAS can extend the growing HA chain, compromising the MW of the produced HA in *B. subtilis*.

Maintaining the DO above a critical level of ~5% saturation was essential to maximize the HA yield in *S. zooepidemicus* cultivations [10], and this is expected given that three mol ATP are required to produce one mol HA disaccharide [2]. While evidence exists to suggest that *B. subtilis* is a facultative anaerobe which uses nitrate as an electron acceptor [145, 146], our attempts to grow 1A751 anaerobically were unsuccessful (unpublished data), indicating that this strain may require a more oxygenic condition to achieve optimal growth. In our study, only supplementation of *n*-hexadecane resulted in DO levels that exceeded 5% saturation throughout the cultivation. Nonetheless, supplementation of *n*-hexadecane, *n*-heptane, perfluoro-1,3,-dimethylcyclohexane, and perfluoromethyldecalin resulted in improvements to the HA titer.

Interestingly, the HA titer was lower in cultures containing 1% v/v *n*-hexadecane, compared to 1% v/v perfluoro-1,3,-dimethylcyclohexane or perfluoromethyldecalin, in spite of significantly higher DO levels when *n*-hexadecane was present. Manipulation of the *n*-hexadecane concentration led to further increases to the DO level, particularly between 6 and 12 h, although the final HA titer was not significantly higher than that obtained in cultivations containing perfluoro-1,3-dimethylcyclohexane or perfluoromethyldecalin. As a result, we cultivated AW009 under a higher agitation rate of 600 rpm with or without *n*-hexadecane to investigate the individual effects of increased DO levels and *n*-hexadecane addition. The HA titer increased by 245% (3423 mg/L; Figure 17A) after 10 h and the peak MW at 6 h increased by 58% (1.94 MDa; Figure 17B) upon increasing the agitation rate from 300 to 600 rpm with no vector. Cultivation with 0.5% v/v *n*-hexadecane at 600 rpm further increased the HA titer by 30% (4,462 mg/L; Figure 17A), although the MW was 12% lower (1.71 MDa; Figure 17B), compared to the cultivation at 600 rpm with no vector. As was the case at 300 rpm, the final cell density was improved upon the addition of *n*-hexadecane, i.e. OD_{600} 27 for 0.5% v/v *n*-hexadecane vs. OD_{600} 22.1 for the control with no vector (Figure 17C), although the DO profiles were not significantly different (Figure 17D). Moreover, increasing the *n*-hexadecane concentration to 1% v/v during cultivation at 600 rpm reduced the MW by an additional 30%, compared to 0.5% v/v *n*-hexadecane, although DO levels were markedly increased and the final cell density was slightly higher (data not shown).

While our results show that *n*-hexadecane does not impede cell growth in the concentration range up to 2% v/v, the effects of *n*-hexadecane on HA production may be somewhat polar in nature. Streptococcal HAS is an integral membrane protein for autonomous

HA synthesis, which is a process requiring as many as seven different functions for initiation, elongation, and secretion of the HA chain [147]. The relatively small size and few transmembrane domains of streptococcal HAS suggest that they cannot facilitate pore formation for translocation of the growing HA chain [147], and cardiolipin or other lipids may assist HAS in creating an internal pore for HA translocation [115, 148]. Moreover, interactions between cardiolipin and HA may add to the net retention force that keeps the HA-UDP/HAS complex together during polymerization until a sufficient opposing force exceeds the net retention force, resulting in the release of the growing HA chain [149, 150]. The use of *n*-hexadecane as an oxygen vector resulted in significant increases to the HA titer in this work, and in a prior study in which HA was produced in the native production host *S. zooepidemicus* [11]. Accordingly, the enhanced HA production upon supplementation of *n*-hexadecane may not be associated with the catalytic activities of HAS, but the increased ATP generation resulting from increased oxygen transfer [151]. On the other hand, the lower MW of HA produced in cultures containing *n*-hexadecane suggests premature release of the HA chain. Longer alkanes such as *n*-hexadecane can align parallel to the acyl chains in the lipid bilayer, and, therefore, affect acyl chain packing and tilt, resulting in a reduction in the projected area occupied per lipid molecule and an overall increase in the degree of ordering of the lipid bilayer [152, 153]. In our study, penetration of *n*-hexadecane through the cell membrane of AW009 may result in the reordering of lipid acyl chains in the lipid bilayer, in turn, altering their interaction with SeHAS. As a result, the HA-binding regions that retain and coordinate translocation of the growing HA chain, and the pore-like structure through which the chain is extruded may be altered, resulting in lower MW HA.

In addition to the reordering of lipids in the bilayer, exposure to organic solvents can alter the fatty acid and lipid composition of the cell membrane. For example, insertion of long chain alcohols (>C5) into a lipid bilayer can increase membrane fluidity [154, 155], and an increase in the abundance of saturated fatty acids has been observed in the cell membrane of *E. coli* upon exposure to C5-C8 alcohols [156]. Conversely, exposure to ethanol resulted in an increase in unsaturated fatty acids, presumably to compensate for a reduction in membrane fluidity in *E. coli* [156]. Moreover, an increase in either saturated or unsaturated fatty acids has been reported for *E. coli* exposed to a number of other organic solvents [157]. In some cases, the shift in cellular fatty acid composition coincided with changes in the ratio of the major lipids phosphatidylglycerol and phosphatidylethanolamine, while certain solvents caused a dramatic increase in the cardiolipin content [157]. Considering that the functional expression of HAS is dependent on its orientation with certain lipids in the cell membrane (i.e. a strong preference for cardiolipin has been observed *in vitro*) [150], it is possible that alterations to the lipid content of the cell membrane of AW009 via exposure to various oxygen vectors could modulate the functional expression of SeHAS. Furthermore, the composition of cardiolipin acyl chains affected SeHAS activity *in vitro* [138, 144], such that a shift in acyl chain composition of lipids in the cell membrane may also affect the functional expression of SeHAS and, in turn, HA production.

The spreading coefficient (S_{vw}) is an indicator of the spreading characteristics of a given compound, and spreading behavior is anticipated when $S_{vw} > 0$ [89]. While measurements of S_{vw} tend to vary, there is agreement that S_{vw} decreases with increasing size and branching or methylation of the molecule [7, 94, 95]. *n*-heptane is reportedly a spreading vector [7, 139],

while *n*-hexadecane may be a spreading [139] or non-spreading [94] vector. Given the significant molecular size difference between the two vectors, *n*-heptane is more prone to spreading than *n*-hexadecane, such that oxygen transfer was more likely to improve upon the addition of *n*-hexadecane at the low concentrations employed in our study. However, our estimates of k_La suggest that the specific rate of oxygen transfer was nearly identical at the respective optimal concentration of each vector, i.e. 21.8 h^{-1} for 0.5% v/v *n*-hexadecane (Figure 16A) vs. 22 h^{-1} for 0.4% v/v *n*-heptane (Figure 16B), both of which are slightly lower than k_La with no vector (22.9 h^{-1}; Figure 16). The reduced k_La in the presence of *n*-hexadecane could be due to an increased time needed to reach oxygen saturation in the bulk liquid, and this was observed during the application of silicone rubber, a compound with a high affinity for oxygen, as a solid oxygen vector [74]. In any case, the specific rate of oxygen transfer is not the sole determinant of culture performance for HA production, given that the HA titers and cell densities were higher in cultures containing the optimal concentration of *n*-hexadecane, compared to perfluoromethyldecalin, at both 300 rpm and 600 rpm. Furthermore, the relative affinities for oxygen between vectors do not correspond to culture performance, as the respective oxygen solubilities of *n*-heptane and perfluoromethyldecalin are ~80% and 100% higher than *n*-hexadecane [128, 134]. Consequently, alternate factors specific to cell physiology may contribute to the net effects of oxygen vectors on culture performance, and this is underlined by the observation that adding *n*-hexadecane to cultures in different growth phases, i.e. stationary at 0 h and exponential at 2 h, has a dramatic effect on culture performance (Figures 12A-D). As previously mentioned, longer alkanes such as *n*-hexadecane can align parallel to the acyl chains in the lipid bilayer, affecting acyl chain packing and tilt for an overall

increase in the ordering of the lipid bilayer [152, 153]. On the other hand, the interactions between smaller alkanes (e.g. *n*-heptane) and acyl chains disturb the interactions between acyl chains and, in turn, reduce the ordering of the lipid bilayer [152]. The net effect on the structure of the lipid bilayer of AW009 may partially explain the difference in culture performance, which seems to be largely dependent on cell growth, based on the highly similar specific HA titers of 91.7 mg/(L·OD_{600}) and 93.9 mg/(L·OD_{600}) obtained in cultivations containing optimal concentrations of *n*-hexadecane and *n*-heptane, respectively. In the case of perfluorocarbons, membrane uptake of them is slow compared to hydrocarbons due to their relatively high lipophobicity [158], such that partitioning of perfluoromethyldecalin into the lipid bilayer may be less extensive compared to hydrocarbon vectors. Accordingly, increased oxygen transfer may be the most significant factor enhancing culture performance with the presence of perfluoromethyldecalin and perfluoro-1,3-dimethylcyclohexane.

Evidence suggests that excessive shear stress due to high agitation rates can be detrimental to the MW of HA produced in *S. zooepidemicus* cultures [11, 68, 111]. The MW increased from 1.69 MDa to 2.01 MDa as the agitation rate increased from 150 rpm to 450 rpm, while at 700 rpm the MW declined to 1.84 MDa [68]. However, the DO was not held constant during respective experiments at different agitation rates, and it was hypothesized that the lower oxygen transfer rate at 150 rpm negatively affected the MW [68]. Similarly, we observed a 58% increase in the MW of HA produced by AW009 as the agitation rate increased from 300 rpm to 600 rpm. To distinguish between the effects of shear stress and enhanced oxygen transfer, AW009 was cultivated at 300 rpm with supplemental oxygen to maintain the DO concentration at 20 ± 5% saturation (with no vector) to ensure operation above the critical DO

level. The peak MW was within 3% (1.88 MDa; Figure 17B) and the final cell density was 9% higher (OD_{600} 24; Figure 17C), although the titer was 37% lower (2141 mg/L; Figure 17A) compared to the cultivation at 600 rpm with no vector. Based on these observations, it appears that a higher shear rate is not detrimental to the MW of HA produced by *B. subtilis* in batch cultivations operated up to 600 rpm and, in fact, may be beneficial in maximizing the HA titer. Maximum growth rates corresponding to optimal agitation rates have been observed in cultures of various microorganisms [159, 160], although the maximum growth rate also corresponded to a maximum oxygen uptake rate in *Brevibacterium flavum* [160]. In our study, oxygen uptake is not limiting in cultivations operated at 300 rpm with supplemental oxygen, suggesting that either a higher shear rate improved flux through the HA biosynthetic pathway, or excess DO levels were detrimental to the functional expression of SeHAS or carbon flux for HA production. An increase in the specific growth rate, cell density, and expression of certain extracellular enzymes was observed with increasing shear rates in *B. subtilis* cultures [161], indicating that a higher agitation rate could contribute to the higher growth rate and increased HA synthesis observed during operation at 600 rpm with no vector. On the other hand, excess DO can reduce the yields of certain recombinant proteins via oxidation of Met and Cys residues [21], resulting in misfolding, loss of activity, and protease degradation [112, 113]. Throughout much of the cultivation in our study, pure oxygen was needed to maintain the desired DO level. However, the peak MW of HA did not decrease when operating at 300 rpm with supplemental oxygen. While the functional expression of SeHAS could still be affected by pure oxygen feeding, the control of chain length and polymerizing activity are independent functions of SeHAS that are not coupled to one another [149]. Accordingly, further investigation is required

to elucidate the effects of shear stress and DO levels in cultivations of HA-producing *B. subtilis*. In addition, our results suggest that operating at agitation rates in excess of 300 rpm can enhance the MW and HA titer, and that oxygen vectors can further enhance culture performance under these conditions.

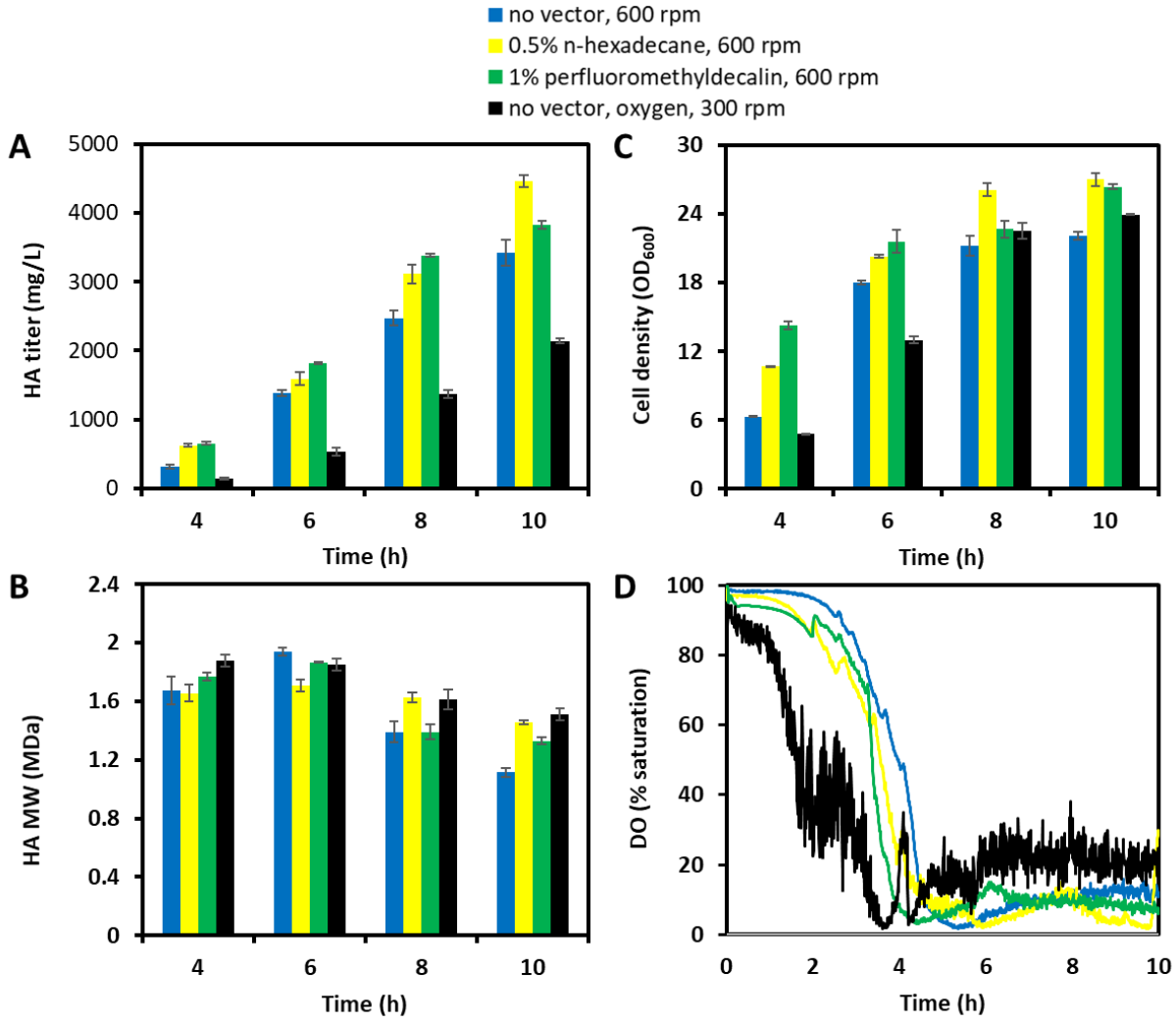

Figure 17: Time profiles of A) HA titer, B) HA MW, C) cell density, and D) DO in cultures of AW009. Experimental conditions: no vector and 600 rpm; 0.5% v/v *n*-hexadecane and 600 rpm; 1% v/v perfluoromethyldecalin and 600 rpm; or no vector, 300 rpm, and supplemental oxygen to maintain the DO concentration at 20 ± 5% saturation. Oxygen vectors were added 2 h after inoculation. SD of duplicate samples shown in Panels A, B,

and C.

Few reports exist on the application of oxygen vectors to microbial HA production or biopolymer production in *B. subtilis.* The application of 0.5% v/v *n*-hexadecane to cultivations of *S. zooepidemicus* for HA production resulted in a similar increase to the HA titer as observed in our work [11]. However, the highest reported MW of 15.4 MDa in the cited study is far in excess of any reported MWs to date, such that comparison of MW data may be not be reasonable. *n*-Dodecane has also been applied to cultivations of *S. zooepidemicus* for enhanced HA production [114]. The addition of 5% v/v *n*-dodecane resulted in a 25% increase in the HA titer, although the maximum increase in MW of 46% was obtained at a concentration of 3% v/v *n*-dodecane, with the peak MW reaching 1.9 MDa [114]. Perfluorodecalin has also been used to enhance HA production in cultures of *S. zooepidemicus,* although the MW was not assessed [22]. The addition of perfluorodecalin to 3% v/v resulted in a 32% improvement to the HA titer, compared to a three phase agitation strategy in which the agitation speed was increased from 200 rpm to 600 rpm, and a further increase in the perfluorodecalin concentration reduced DO levels presumably due to an increase in culture viscosity [22]. While the application of oxygen vectors to cultivations of *S. zooepidemicus* result in relative increases in the HA titer similar to our cultivations with *B. subtilis*, the improvements to the MW suggest that the functional expression of native HAS may be less sensitive to perturbations that may affect cell membrane ordering and fluidity. *n*-Heptane and *n*-hexadecane have also been applied as oxygen vectors to PGA production in cultures of *B. subtilis* [23], resulting in respective increases in the titer of 25% and 20%, as well as respective increases in the MWs of 25% and 20%. PgsB and PgsC, which are the capsular PGA synthetase and capsular PGA

amide ligase/translocase subunit, respectively, polymerize PGA, which is presumably translocated out of the cell by CapA and PgsE (whose respective functions have not been formally elucidated) with assistance from PgsC [162]. Accordingly, at least four proteins are involved in the synthesis and translocation of PGA in *B. subtilis*, and this is in contrast to HA production for which a single enzyme (i.e. HAS) is responsible [147]. Due to the autonomous functionality of SeHAS, which is dependent on its orientation with lipids in the cell membrane [115, 148], reordering or alteration of lipids in the cell membrane may have a more pronounced impact on the functional expression of SeHAS, but not the elaborate PGA-producing enzyme complex. This potentially results in markedly different effects on the MW of different biopolymers.

Chapter 4- Conclusions

The comparative analysis presented herein demonstrates the utility of oxygen vectors in obtaining typical biopolymer (HA) yields in batch cultures. Here, we report the application of oxygen vectors to the heterologous production of HA in engineered *Bacillus subtilis*, leading to significantly improved culture performance. Out of seven potential oxygen vectors evaluated in a preliminary screening, significant improvements to the HA titer and/or cell density were observed in cultures containing *n*-heptane, *n*-hexadecane, perfluoromethyldecalin, and perfluoro-1,3-dimethylcyclohexane. Notably, *n*-hexadecane was the only compound tested that provided a substantial increase in DO levels, which remained above 10% saturation throughout the cultivation (Figure 11D). Our results indicate that certain vectors may alter the functional expression of Class I hyaluronan synthase (HAS) in *B. subtilis*. The functional expression of HAS to maximize HA production is dependent on its specific orientation with certain lipids in the cell membrane. Streptococcal HAS is an integral membrane protein for autonomous HA synthesis, which is a process requiring as many as seven different functions for initiation, elongation, and secretion of the HA chain. The relatively small size and few transmembrane domains of streptococcal HAS suggest that they cannot facilitate pore formation for translocation of the growing HA chain, and cardiolipin or other lipids may assist HAS in creating an internal pore for HA translocation. Moreover, interactions between cardiolipin and HA may add to the net retention force that keeps the HA-UDP/HAS complex together during polymerization until a sufficient opposing force exceeds the net retention force, resulting in the release of the growing HA chain. Longer alkanes such as *n*-hexadecane can align parallel to

the acyl chains in the lipid bilayer, and, therefore, affect acyl chain packing and tilt, resulting in a reduction in the projected area occupied per lipid molecule and an overall increase in the degree of ordering of the lipid bilayer. The insertion of long chain alcohols (>C5) into a lipid bilayer can increase membrane fluidity. It is possible that alterations to the lipid content of the cell membrane of AW009 via exposure to various oxygen vectors could modulate the functional expression of SeHAS. Furthermore, the composition of cardiolipin acyl chains affected SeHAS activity *in vitro*, such that a shift in acyl chain composition of lipids in the cell membrane may also affect the functional expression of SeHAS and, in turn, HA production. The interactions between smaller alkanes (e.g. *n*-heptane) and acyl chains disturb the interactions between acyl chains and, in turn, reduce the ordering of the lipid bilayer. The net effect on the structure of the lipid bilayer of AW009 may partially explain the difference in culture performance, which seems to be largely dependent on cell growth, based on the highly similar specific HA titers of 91.7 mg/(L·OD_{600}) and 93.9 mg/(L·OD_{600}) obtained in cultivations containing optimal concentrations of *n*-hexadecane and *n*-heptane, respectively. In the case of perfluorocarbons, membrane uptake of them is slow compared to hydrocarbons due to their relatively high lipophobicity, such that partitioning of perfluoromethyldecalin into the lipid bilayer may be less extensive compared to hydrocarbon vectors. Accordingly, increased oxygen transfer may be the most significant factor enhancing culture performance with the presence of perfluoromethyldecalin and perfluoro-1,3-dimethylcyclohexane.

Higher shear rates may drive more carbon flux through the HA biosynthetic pathway without negatively affecting the MW. Based on these observations, it appears that a higher shear rate is not detrimental to the MW of HA produced by *B. subtilis* in batch cultivations

operated up to 600 rpm and, in fact, may be beneficial in maximizing the HA titer. Our results suggest that operating at agitation rates in excess of 300 rpm can enhance the MW and HA titer, and that oxygen vectors can further enhance culture performance under these conditions. Due to the autonomous functionality of SeHAS, which is dependent on its orientation with lipids in the cell membrane, reordering or alteration of lipids in the cell membrane may have a more pronounced impact on the functional expression of SeHAS, potentially resulting in markedly different effects on the MW compared with other several-enzyme driving biopolymers.

Adjustments to the vector concentration, timing of vector addition, and the agitation rate resulted in further enhancements, with the HA titer reaching up to 4.5 g/L after only 10 h cultivation. Our study demonstrates the efficacy of oxygen vectors to enhance heterologous HA production in *B. subtilis*, and provides valuable insight for future bioprocess development in microbial HA production. It is possible that the usage of proper oxygen vectors in the future studies and industry can obtain a relatively substantial improvement of the quality and quantity of bioproducts.

Reference

[1] B. F. Chong, L. M. Blank, R. Mclaughlin, and L. K. Nielsen, "Microbial hyaluronic acid production," *Applied microbiology and biotechnology,* vol. 66, pp. 341-351, 2005.

[2] B. Widner, R. Behr, S. Von Dollen, M. Tang, T. Heu, A. Sloma*, et al.*, "Hyaluronic acid production in Bacillus subtilis," *Applied and environmental microbiology,* vol. 71, pp. 3747-3752, 2005.

[3] L. Liu, Y. Liu, J. Li, G. Du, and J. Chen, "Microbial production of hyaluronic acid: current state, challenges, and perspectives," *Microbial cell factories,* vol. 10, p. 99, 2011.

[4] L. Liu, Y. Liu, J. Li, G. Du, and J. Chen, "Microbial production of hyaluronic acid: current state, challenges, and perspectives," *Microbial Cell Factories,* vol. 10, pp. 1-9, 2011.

[5] F. Garcia-Ochoa and E. Gomez, "Bioreactor scale-up and oxygen transfer rate in microbial processes: An overview," *Biotechnology Advances,* vol. 27, pp. 153-176, 3// 2009.

[6] *Developments and Applications in Solubility*, 1 ed.: Royal Society of Chemistry, 2007.

[7] H. J. Pinho and S. S. Alves, "Effect of spreading coefficient on gas-liquid mass transfer in gas-liquid-liquid dispersions in a stirred tank," *Chemical Engineering Communications,* vol. 197, pp. 1515-1526, 2010.

[8] C. Van Ede, R. Van Houten, and A. Beenackers, "Enhancement of gas to water mass transfer rates by a dispersed organic phase," *Chemical engineering science,* vol. 50, pp. 2911-2922, 1995.

[9] Z. Zhang, W. Chen, S. Yu, and W. Li, "Enhancement of gas-to-water mass-transfer rates

by the second liquid phase," *Industrial & Engineering Chemistry Research,* vol. 49, pp. 3223-3227, 2010.

[10] W.-C. Huang, S.-J. Chen, and T.-L. Chen, "The role of dissolved oxygen and function of agitation in hyaluronic acid fermentation," *Biochemical Engineering Journal,* vol. 32, pp. 239-243, 2006.

[11] Z.-W. Lai, R. A. Rahim, A. B. Ariff, and R. Mohamad, "Biosynthesis of high molecular weight hyaluronic acid by *Streptococcus zooepidemicus* using oxygen vector and optimum impeller tip speed," *Journal of Bioscience and Bioengineering,* vol. 114, pp. 286-291, 9// 2012.

[12] T. L. Da Silva, V. Calado, N. Silva, R. L. Mendes, S. S. Alves, J. M. Vasconcelos*, et al.*, "Effects of hydrocarbon additions on gas-liquid mass transfer coefficients in biphasic bioreactors," *Biotechnology and Bioprocess Engineering,* vol. 11, pp. 245-250, 2006.

[13] E. Nagy, "Three-phase mass transfer: one-dimensional heterogeneous model," *Chemical engineering science,* vol. 50, pp. 827-836, 1995.

[14] E. Dumont and H. Delmas, "Mass transfer enhancement of gas absorption in oil-in-water systems: a review," *Chemical Engineering and Processing: Process Intensification,* vol. 42, pp. 419-438, 6// 2003.

[15] L. Correia, C. Aldrich, and K. Clarke, "Interfacial gas–liquid transfer area in alkane–aqueous dispersions and its impact on the overall volumetric oxygen transfer coefficient," *Biochemical engineering journal,* vol. 49, pp. 133-137, 2010.

[16] A.-I. Galaction, D. Cascaval, C. Oniscu, and M. Turnea, "Prediction of oxygen mass transfer coefficients in stirred bioreactors for bacteria, yeasts and fungus broths,"

Biochemical Engineering Journal, vol. 20, pp. 85-94, 2004.

[17] G. Quijano, J. Rocha-Ríos, M. Hernández, S. Villaverde, S. Revah, R. Muñoz*, et al.*, "Determining the effect of solid and liquid vectors on the gaseous interfacial area and oxygen transfer rates in two-phase partitioning bioreactors," *Journal of hazardous materials,* vol. 175, pp. 1085-1089, 2010.

[18] H. Chaumat, A. M. Billet, and H. Delmas, "Hydrodynamics and mass transfer in bubble column: Influence of liquid phase surface tension," *Chemical Engineering Science,* vol. 62, pp. 7378-7390, 12// 2007.

[19] G. Quijano, M. Hernandez, S. Villaverde, F. Thalasso, and R. Muñoz, "A step-forward in the characterization and potential applications of solid and liquid oxygen transfer vectors," *Applied microbiology and biotechnology,* vol. 85, pp. 543-551, 2010.

[20] H. Hristov, R. Mann, V. Lossev, S. D. Vlaev, and P. Seichter, "A 3-D analysis of gas-liquid mixing, mass transfer and bioreaction in a stirred bio-reactor," *Food and Bioproducts Processing,* vol. 79, pp. 232-241, 2001.

[21] S. B. Farr and T. Kogoma, "Oxidative stress responses in *Escherichia coli* and *Salmonella typhimurium*," *Microbiological Reviews,* vol. 55, pp. 561-585, December 1, 1991 1991.

[22] L. Liu, G. Du, J. Chen, M. Wang, and J. Sun, "Comparative study on the influence of dissolved oxygen control approaches on the microbial hyaluronic acid production of Streptococcus zooepidemicus," *Bioprocess and biosystems engineering,* vol. 32, pp. 755-763, 2009.

[23] D. Zhang, X. Feng, S. Li, F. Chen, and H. Xu, "Effects of oxygen vectors on the

synthesis and molecular weight of poly(γ-glutamic acid) and the metabolic characterization of Bacillus subtilis NX-2," *Process Biochemistry,* vol. 47, pp. 2103-2109, 12// 2012.

[24] Z. Xu, F. Bo, J. Xia, Z. Sun, S. Li, X. Feng*, et al.*, "Effects of oxygen-vectors on the synthesis of epsilon-poly-lysine and the metabolic characterization of Streptomyces albulus PD-1," *Biochemical Engineering Journal,* vol. 94, pp. 58-64, 2015.

[25] M. Pilarek, J. Glazyrina, and P. Neubauer, "Enhanced growth and recombinant protein production of Escherichia coli by a perfluorinated oxygen carrier in miniaturized fed-batch cultures," *Microbial Cell Factories,* vol. 10, pp. 1-9, 2011.

[26] W. G. Whitman, "The two film theory of gas absorption," *International Journal of Heat and Mass Transfer,* vol. 5, pp. 429-433, 1962.

[27] F. Garcia-Ochoa and E. Gomez, "Bioreactor scale-up and oxygen transfer rate in microbial processes: an overview," *Biotechnology advances,* vol. 27, pp. 153-176, 2009.

[28] H. Toor and J. Marchello, "Film - penetration model for mass and heat transfer," *AIChE Journal,* vol. 4, pp. 97-101, 1958.

[29] R. Higbie, *The rate of absorption of a pure gas into still liquid during short periods of exposure*, 1935.

[30] S. Sideman, "The equivalence of the penetration and potential flow theories," *Industrial & Engineering Chemistry,* vol. 58, pp. 54-58, 1966.

[31] F. Garcia-Ochoa, V. E. Santos, and E. Gomez, "2.15 - Stirred Tank Bioreactors," in *Comprehensive Biotechnology (Second Edition)*, M. Moo-Young, Ed., ed Burlington: Academic Press, 2011, pp. 179-198.

[32] M. M. L. de Figueiredo and P. H. Calderbank, "The scale-up of aerated mixing vessels for specified oxygen dissolution rates," *Chemical Engineering Science,* vol. 34, pp. 1333-1338, 1979.

[33] V. Linek and V. Vacek, "Volumetric mass transfer coefficient in stirred reactors," *Chemical Engineering & Technology,* vol. 11, pp. 249-251, 1988.

[34] K. Van't Riet, "Review of measuring methods and results in nonviscous gas-liquid mass transfer in stirred vessels," *Industrial & Engineering Chemistry Process Design and Development,* vol. 18, pp. 357-364, 1979.

[35] F. García-Ochoa and E. G. Castro, "Estimation of oxygen mass transfer coefficient in stirred tank reactors using artificial neural networks," *Enzyme and Microbial Technology,* vol. 28, pp. 560-569, 2001.

[36] M. Nishikawa, M. Nakamura, H. Yagi, and K. Hashimoto, "Gas absorption in aerated mixing vessels," *Journal of Chemical Engineering of Japan,* vol. 14, pp. 219-226, 1981.

[37] A. Ogut and R. T. Hatch, "Oxygen transfer into newtonian and non-newtonian fluids in mechanically agitated vessels," *The Canadian Journal of Chemical Engineering,* vol. 66, pp. 79-85, 1988.

[38] F. García-Ochoa and E. Gómez, "Mass transfer coefficient in stirred tank reactors for xanthan gum solutions," *Biochemical Engineering Journal,* vol. 1, pp. 1-10, 1998.

[39] H. Yagi and F. Yoshida, "Gas absorption by Newtonian and non-Newtonian fluids in sparged agitated vessels," *Industrial & Engineering Chemistry Process Design and Development,* vol. 14, pp. 488-493, 1975/10/01 1975.

[40] J. F. Perez and O. C. Sandall, "Gas absorption by non-Newtonian fluids in agitated

vessels," *AIChE Journal,* vol. 20, pp. 770-775, 1974.

[41] F. Garcia-Ochoa and E. Gomez, "Theoretical prediction of gas–liquid mass transfer coefficient, specific area and hold-up in sparged stirred tanks," *Chemical Engineering Science,* vol. 59, pp. 2489-2501, 2004.

[42] M. Tobajas, E. García-Calvo, M. H. Siegel, and S. E. Apitz, "Hydrodynamics and mass transfer prediction in a three-phase airlift reactor for marine sediment biotreatment," *Chemical Engineering Science,* vol. 54, pp. 5347-5354, 1999.

[43] A. B. Pandit and J. B. Joshi, "Mixing in mechanically agitated gas-liquid contactors, bubble columns and modified bubble columns," *Chemical Engineering Science,* vol. 38, pp. 1189-1215, 1983.

[44] A. Mandal, G. Kundu, and D. Mukherjee, "Gas-holdup distribution and energy dissipation in an ejector-induced downflow bubble column: the case of non-Newtonian liquid," *Chemical engineering science,* vol. 59, pp. 2705-2713, 2004.

[45] N. Kantarci, F. Borak, and K. O. Ulgen, "Bubble column reactors," *Process Biochemistry,* vol. 40, pp. 2263-2283, 2005.

[46] K. Agrawal, "Bubble dynamics and interface phenomenon," *Journal of Engineering and Technology Research,* vol. 5, pp. 42-50, 2013.

[47] P. M. Kilonzo and A. Margaritis, "The effects of non-Newtonian fermentation broth viscosity and small bubble segregation on oxygen mass transfer in gas-lift bioreactors: a critical review," *Biochemical Engineering Journal,* vol. 17, pp. 27-40, 2004.

[48] C. L. Hyndman, F. Larachi, and C. Guy, "Understanding gas-phase hydrodynamics in bubble columns: a convective model based on kinetic theory," *Chemical engineering*

science, vol. 52, pp. 63-77, 1997.

[49] A. Schumpe and G. Grund, "The gas disengagement technique for studying gas holdup structure in bubble columns," *The Canadian Journal of Chemical Engineering,* vol. 64, pp. 891-896, 1986.

[50] B. Thorat and J. Joshi, "Regime transition in bubble columns: experimental and predictions," *Experimental Thermal and Fluid Science,* vol. 28, pp. 423-430, 2004.

[51] K. Kawagoe, T. Inoue, K. Nakao, and T. Otake, "Flow-Pattern and Gas-Holdup Conditions in Gas-Sparged Contactors," *International Chemical Engineering,* vol. 16, pp. 176-183, 1976.

[52] R. Krishna and J. Van Baten, "Mass transfer in bubble columns," *Catalysis Today,* vol. 79, pp. 67-75, 2003.

[53] K. Van't Riet and J. Tramper, *Basic bioreactor design*: CRC Press, 1991.

[54] H. Lange, P. Taillandier, and J. P. Riba, "Effect of high shear stress on microbial viability," *Journal of Chemical Technology and Biotechnology,* vol. 76, pp. 501-505, 2001.

[55] B. Gorain, J.-P. Franzidis, and E. Manlapig, "Studies on impeller type, impeller speed and air flow rate in an industrial scale flotation cell—Part 1: Effect on bubble size distribution," *Minerals Engineering,* vol. 8, pp. 615-635, 1995.

[56] B. Gorain, J.-P. Franzidis, and E. Manlapig, "Studies on impeller type, impeller speed and air flow rate in an industrial scale flotation cell. Part 3: Effect on superficial gas velocity," *Minerals Engineering,* vol. 9, pp. 639-654, 1996.

[57] B. Gorain, J.-P. Franzidis, and E. Manlapig, "Studies on impeller type, impeller speed

and air flow rate in an industrial scale flotation cell part 2: Effect on gas holdup," *Minerals Engineering,* vol. 8, pp. 1557-1570, 1995.

[58] M. S. Puthli, V. K. Rathod, and A. B. Pandit, "Gas–liquid mass transfer studies with triple impeller system on a laboratory scale bioreactor," *Biochemical Engineering Journal,* vol. 23, pp. 25-30, 2005.

[59] Y. Zhu, P. C. Bandopadhayay, and J. Wu, "Measurement of Gas-Liquid Mass Transfer in an Agitated Vessel. A Comparison between Different Impellers," *Journal of chemical engineering of Japan,* vol. 34, pp. 579-584, 2001.

[60] W.-D. Deckwer, Y. Louisi, A. Zaidi, and M. Ralek, "Hydrodynamic properties of the Fischer-Tropsch slurry process," *Industrial & Engineering Chemistry Process Design and Development,* vol. 19, pp. 699-708, 1980.

[61] S. Saxena, N. Rao, and A. Saxena, "Heat-transfer and gas-holdup studies in a bubble column: air-water-glass bead system," *Chemical engineering communications,* vol. 96, pp. 31-55, 1990.

[62] Y. Shah, B. G. Kelkar, S. Godbole, and W. D. Deckwer, "Design parameters estimations for bubble column reactors," *AIChE Journal,* vol. 28, pp. 353-379, 1982.

[63] R. Krishna, J. W. De Swart, J. Ellenberger, G. B. Martina, and C. Maretto, "Gas holdup in slurry bubble columns: effect of column diameter and slurry concentrations," *AIChE Journal,* vol. 43, pp. 311-316, 1997.

[64] R. Krishna, J. W. De Swart, D. E. Hennephof, J. Ellenberger, and H. C. Hoefsloot, "Influence of increased gas density on hydrodynamics of bubble‐column reactors," *AIChE journal,* vol. 40, pp. 112-119, 1994.

[65] R. Krishna, P. Wilkinson, and L. Van Dierendonck, "A model for gas holdup in bubble columns incorporating the influence of gas density on flow regime transitions," *Chemical Engineering Science,* vol. 46, pp. 2491-2496, 1991.

[66] X. Luo, D. Lee, R. Lau, G. Yang, and L. S. Fan, "Maximum stable bubble size and gas holdup in high‐pressure slurry bubble columns," *AIChE Journal,* vol. 45, pp. 665-680, 1999.

[67] M. Bouaifi, G. Hebrard, D. Bastoul, and M. Roustan, "A comparative study of gas hold-up, bubble size, interfacial area and mass transfer coefficients in stirred gas–liquid reactors and bubble columns," *Chemical Engineering and Processing: Process Intensification,* vol. 40, pp. 97-111, 2001.

[68] X.-J. Duan, L. Yang, X. Zhang, and W.-S. Tan, "Effect of oxygen and shear stress on molecular weight of hyaluronic acid," *Journal of Microbiology and Biotechnology,* vol. 18, pp. 718-724, 2008.

[69] T. L. da Silva, V. Calado, N. Silva, R. L. Mendes, S. S. Alves, J. M. T. Vasconcelos*, et al.*, "Effects of hydrocarbon additions on gas-liquid mass transfer coefficients in biphasic bioreactors," *Biotechnology and Bioprocess Engineering,* vol. 11, pp. 245-250, 2006.

[70] J. L. Rols, J. S. Condoret, C. Fonade, and G. Goma, "Modeling of oxygen transfer in water through emulsified organic liquids," *Chemical Engineering Science,* vol. 46, pp. 1869-1873, 1991/01/01 1991.

[71] J. L. Rols, J. S. Condoret, C. Fonade, and G. Goma, "Mechanism of Enhanced Oxygen Transfer in Fermentation Using Emulsified Oxygen-Vectors," *BIOTECHNOLOGY*

AND BIOENGINEERING vol. 35, February 1990 1990.

[72] M. Elibol, "Improvement of antibiotic production by increased oxygen solubility through the addition of perfluorodecalin," *Journal of Chemical Technology & Biotechnology,* vol. 76, pp. 418-422, 2001.

[73] J. L. Rols and G. Goma, "Enhanced oxygen transfer rates in fermentation using soybean oil-in-water dispersions," *Biotechnology Letters,* vol. 13, pp. 7-12, 1991// 1991.

[74] J. V. Littlejohns and A. J. Daugulis, "Oxygen transfer in a gas–liquid system containing solids of varying oxygen affinity," *Chemical Engineering Journal,* vol. 129, pp. 67-74, 2007.

[75] J. V. Littlejohns and A. J. Daugulis, "Oxygen transfer in a gas–liquid system containing solids of varying oxygen affinity," *Chemical Engineering Journal,* vol. 129, pp. 67-74, 2007.

[76] C. J. Van Ede, R. Van Houten, and A. A. C. M. Beenackers, "Enhancement of gas to water mass transfer rates by a dispersed organic phase," *Chemical Engineering Science,* vol. 50, pp. 2911-2922, 1995/09/01 1995.

[77] L. D. C. Correia, C. Aldrich, and K. G. Clarke, "Interfacial gas–liquid transfer area in alkane–aqueous dispersions and its impact on the overall volumetric oxygen transfer coefficient," *Biochemical Engineering Journal,* vol. 49, pp. 133-137, 3/15/ 2010.

[78] C. I. Castro and J. C. Briceno, "Perfluorocarbon-Based Oxygen Carriers: Review of Products and Trials," *Artificial Organs,* vol. 34, pp. 622-634, 2010.

[79] H. J. Reich, "8.1 Relaxation in NMR Spectroscopy, Chem 605 Course Notes," ed. University of Wisconsin, 2010.

[80] M. H. A. Hamza, G. Serratrice, M. J. Stebe, and J. J. Delpuech, "Solute-solvent interactions in perfluorocarbon solutions of oxygen. An NMR study," *Journal of the American Chemical Society,* vol. 103, pp. 3733-3738, 1981/07/01 1981.

[81] M. J. Stebe, G. Serratrice, and J. J. Delpuech, "Fluorocarbons as oxygen carriers. An NMR study of nonionic fluorinated microemulsions and of their oxygen solutions," *The Journal of Physical Chemistry,* vol. 89, pp. 2837-2843, 1985/06/01 1985.

[82] M. H. Ali Hamza, G. Serratrice, M.-J. Stébé, and J.-J. Delpuech, "Fluorocarbons as oxygen carriers. II. An NMR study of partially or totally fluorinated alkanes and alkenes," *Journal of Magnetic Resonance (1969),* vol. 42, pp. 227-241, 1981/02/01 1981.

[83] G. D. Zhang, W. F. Cai, C. J. Xu, and M. Zhou, "A general enhancement factor model of the physical absorption of gases in multiphase systems," *Chemical Engineering Science,* vol. 61, pp. 558-568, 2006.

[84] J. V. Littlejohns and A. J. Daugulis, "Oxygen transfer in a gas–liquid system containing solids of varying oxygen affinity," *Chemical Engineering Journal,* vol. 129, pp. 67-74, 5/1/ 2007.

[85] J. D. McMillan and D. I. C. Wang, "Mechanisms of Oxygen Transfer Enhancement during Submerged Cultivation in Perfluorochemical-in-Water Dispersions," *Annals of the New York Academy of Sciences,* vol. 589, pp. 283-300, 1990.

[86] P. Chen, "ChE 612 course notes, S2016," ed. University of Waterloo, 2016.

[87] D. W. F. Brilman, "Mass transfer and chemical reaction in gas-liquid-liquid systems," PhD, Chemical Engineering, University of Twente, Enschede, The Netherlands, 1998.

[88] J. Stauft, "J. T. Davies und E. K. Rideal. Interfacial Phenomena. Academic Press, New York und London 1961. 474 S. Preis: $ 14,—," *Zeitschrift für Elektrochemie, Berichte der Bunsengesellschaft für physikalische Chemie,* vol. 66, pp. 453-453, 1962.

[89] J. L. Rols, J. S. Condoret, C. Fonade, and G. Goma, "Mechanism of enhanced oxygen transfer in fermentation using emulsified oxygen-vectors," *Biotechnology and Bioengineering,* vol. 35, pp. 427-435, 1990.

[90] D. Brilman, M. Goldschmidt, G. Versteeg, and W. Van Swaaij, "Heterogeneous mass transfer models for gas absorption in multiphase systems," *Chemical Engineering Science,* vol. 55, pp. 2793-2812, 2000.

[91] F. Yoshida, T. Yamane, and Y. Miyamoto, "Oxygen Absorption into Oil-in-Water Emulsions. A Study on Hydrocarbon Fermentors," *Industrial & Engineering Chemistry Process Design and Development,* vol. 9, pp. 570-577, 1970/10/01 1970.

[92] J. Rols, J. Condoret, C. Fonade, and G. Goma, "Mechanism of enhanced oxygen transfer in fermentation using emulsified oxygen‐vectors," *Biotechnology and bioengineering,* vol. 35, pp. 427-435, 1990.

[93] R. Oliveira, G. Gonzalez, and J. Oliveira, "Interfacial studies on dissolved gas flotation of oil droplets for water purification," *Colloids and Surfaces A: Physicochemical and Engineering Aspects,* vol. 154, pp. 127-135, 1999.

[94] I. Hassan and C. W. Robinson, "Oxygen transfer in mechanically agitated aqueous systems containing dispersed hydrocarbon," *Biotechnology and Bioengineering,* vol. 19, pp. 661-682, 1977.

[95] Y. H. Mori, N. Tsui, and M. Kiyomiya, "Surface and interfacial tensions and their

combined properties in seven binary, immiscible liquid-liquid-vapor systems," *Journal of Chemical and Engineering Data,* vol. 29, pp. 407-412, 1984.

[96] S.-Y. Akatsuka, H. Yoshigiwa, and Y. H. Mori, "Temperature dependencies of spreading coefficients of hydrocarbons on water," *Journal of colloid and interface science,* vol. 172, pp. 335-340, 1995.

[97] T. Pfohl and H. Riegler, "Critical wetting of a liquid/vapor interface by octane," *Physical review letters,* vol. 82, p. 783, 1999.

[98] R. L. Kars, R. J. Best, and A. A. H. Drinkenburg, "The sorption of propane in slurries of active carbon in water," *The Chemical Engineering Journal,* vol. 17, pp. 201-210, 1979/01/01/ 1979.

[99] J. Kluytmans, B. Van Wachem, B. Kuster, and J. Schouten, "Mass transfer in sparged and stirred reactors: influence of carbon particles and electrolyte," *Chemical Engineering Science,* vol. 58, pp. 4719-4728, 2003.

[100] K. Ruthiya, J. Van der Schaaf, B. Kuster, and J. Schouten, "Mechanisms of physical and reaction enhancement of mass transfer in a gas inducing stirred slurry reactor," *Chemical Engineering Journal,* vol. 96, pp. 55-69, 2003.

[101] T. R. Das, A. Bandopadhyay, R. Parthasarathy, and R. Kumar, "Gas—liquid interfacial area in stirred vessels: The effect of an immiscible liquid phase," *Chemical Engineering Science,* vol. 40, pp. 209-214, 1985/01/01 1985.

[102] A. H. G. Cents, D. W. F. Brilman, and G. F. Versteeg, "Gas absorption in an agitated gas–liquid–liquid system," *Chemical Engineering Science,* vol. 56, pp. 1075-1083, 2// 2001.

[103] I. T. M. Hassan and C. W. Robinson, "Oxygen transfer in mechanically agitated aqueous systems containing dispersed hydrocarbon," *Biotechnology and Bioengineering,* vol. 19, pp. 661-682, 1977.

[104] V. Linek and P. Beneš, "A study of the mechanism of gas absorption into oil-water emulsions," *Chemical Engineering Science,* vol. 31, pp. 1037-1046, 1976/01/01 1976.

[105] S. Pullman-Mooar, P. Mooar, M. Sieck, G. Clayburne, and H. R. Schumacher, "Are there distinctive inflammatory flares after hylan g-f 20 intraarticular injections?," *The Journal of Rheumatology,* vol. 29, pp. 2611-2614, December 1, 2002 2002.

[106] M. O'Regan, I. Martini, F. Crescenzi, C. De Luca, and M. Lansing, "Molecular mechanisms and genetics of hyaluronan biosynthesis," *International Journal of Biological Macromolecules,* vol. 16, pp. 283-286, 1994/12/01 1994.

[107] J. A. Vázquez, M. I. Montemayor, J. Fraguas, and M. A. Murado, "Hyaluronic acid production by *Streptococcus zooepidemicus* in marine by-products media from mussel processing wastewaters and tuna peptone viscera," *Microbial Cell Factories,* vol. 9, pp. 1-10, 2010// 2010.

[108] M. Schallmey, A. Singh, and O. P. Ward, "Developments in the use of *Bacillus* species for industrial production," *Canadian Journal of Microbiology,* vol. 50, pp. 1-17, 2004/01/01 2004.

[109] J. A. Mueller and W. C. Boyle, "Relative importance of viscosity and oxygen solubility on oxygen transfer rates in glucose solutions," *Environmental Science & Technology,* vol. 1, pp. 578-579, 1967/07/01 1967.

[110] F. García-Ochoa, E. G. Castro, and V. E. Santos, "Oxygen transfer and uptake rates

during xanthan gum production," *Enzyme and Microbial Technology,* vol. 27, pp. 680-690, 11/15/ 2000.

[111] H. Gao, J. Chen, G. Du, Y. Zhang, J. Chen, and G. Chen, "Effect of agitation and mixing on hyaluronic acid production by *Streptococcus zooepidemicus*," *JOURNAL OF CHEMICAL INDUSTRY AND ENGINEERING-CHINA-,* vol. 54, pp. 350-356, 2003.

[112] A. Slavica, I. Dib, and B. Nidetzky, "Single-site oxidation, cysteine 108 to cysteine sulfinic acid, in d-amino acid oxidase from *Trigonopsis variabilis* and its structural and functional consequences," *Applied and Environmental Microbiology,* vol. 71, pp. 8061-8068, December 1, 2005 2005.

[113] R. T. Dean, S. Fu, R. Stocker, and M. J. Davies, "Biochemistry and pathology of radical-mediated protein oxidation.," *Biochemical Journal,* vol. 324, pp. 1-18, 1997.

[114] L. Liu, H. Q. Yang, D. X. Zhang, G. C. Du, J. Chen, M. Wang*, et al.*, "Enhancement of hyaluronic acid production by batch culture of *Streptococcus zooepidemicus* via the addition of n-dodecane as an oxygen vector," *Journal of microbiology and biotechnology,* vol. 19, pp. 596-603, 2009.

[115] A. W. Westbrook, X. Ren, M. Moo‐Young, and C. P. Chou, "Engineering of cell membrane to enhance heterologous production of hyaluronic acid in *Bacillus subtilis*," *Biotechnology and Bioengineering,* 2017.

[116] J. Sambrook and D. Russell, *Molecular cloning: a laboratory manual*: Cold Spring Harbor Laboratory Press, 2001.

[117] A. W. Westbrook, M. Moo-Young, and C. P. Chou, "Development of a CRISPR-Cas9 tool kit for comprehensive engineering of *Bacillus subtilis*," *Appl Environ Microbiol,*

vol. 82, pp. 4876-95, Aug 15 2016.

[118] L.-J. Chien and C.-K. Lee, "Enhanced hyaluronic acid production in *Bacillus subtilis* by coexpressing bacterial hemoglobin," *Biotechnology Progress,* vol. 23, pp. 1017-1022, 2007.

[119] H. Nguyen, T. Phan, and W. Schumann, "Expression vectors for the rapid purification of recombinant proteins in *Bacillus subtilis*," *Current Microbiology,* vol. 55, pp. 89-93, 2007/08/01 2007.

[120] T. T. P. Phan, H. D. Nguyen, and W. Schumann, "Development of a strong intracellular expression system for *Bacillus subtilis* by optimizing promoter elements," *Journal of Biotechnology,* vol. 157, pp. 167-172, 1// 2012.

[121] T. Bitter and H. M. Muir, "A modified uronic acid carbazole reaction," *Analytical Biochemistry,* vol. 4, pp. 330-334, 1962/10/01 1962.

[122] M. K. Cowman, C. C. Chen, M. Pandya, H. Yuan, D. Ramkishun, J. LoBello*, et al.*, "Improved agarose gel electrophoresis method and molecular mass calculation for high molecular mass hyaluronan," *Analytical Biochemistry,* vol. 417, pp. 50-56, 10/1/ 2011.

[123] C. A. Schneider, W. S. Rasband, and K. W. Eliceiri, "NIH Image to ImageJ: 25 years of image analysis," *Nat Meth,* vol. 9, pp. 671-675, 07//print 2012.

[124] W. Y. Chen, E. Marcellin, J. Hung, and L. K. Nielsen, "Hyaluronan molecular weight is controlled by UDP-N-acetylglucosamine concentration in *Streptococcus zooepidemicus*," *Journal of Biological Chemistry,* vol. 284, pp. 18007-18014, 2009.

[125] M. I. Aralaguppi, T. M. Aminabhavi, R. H. Balundgi, and S. S. Joshi, "Thermodynamic interactions in mixtures of bromoform with hydrocarbons," *The Journal of Physical*

Chemistry, vol. 95, pp. 5299-5308, 1991.

[126] L. K. Ju and C. S. Ho, "Oxygen diffusion coefficient and solubility in n‐hexadecane," *Biotechnology and bioengineering,* vol. 34, pp. 1221-1224, 1989.

[127] E. Michailidou, M. J. Assael, M. L. Huber, I. M. Abdulagatov, and R. A. Perkins, "Reference correlation of the viscosity of *n*-heptane from the triple point to 600 K and up to 248 MPa," *Journal of Physical and Chemical Reference Data,* vol. 43, p. 023103, 2014.

[128] A. B. McKeown and R. Hibbard, "Determination of dissolved oxygen in hydrocarbons," *Analytical Chemistry,* vol. 28, pp. 1490-1492, 1956.

[129] P. J. Hesse, R. Battino, P. Scharlin, and E. Wilhelm, "Solubility of gases in liquids. 21. Solubility of He, Ne, Ar, Kr, N 2, O 2, CH 4, CF 4, and SF 6 in 2, 2, 4-trimethylpentane atT= 298.15 K," *The Journal of Chemical Thermodynamics,* vol. 31, pp. 1175-1181, 1999.

[130] A. Pádua, J. Fareleira, J. Calado, and W. Wakeham, "Density and viscosity measurements of 2, 2, 4-trimethylpentane (isooctane) from 198 K to 348 K and up to 100 MPa," *Journal of Chemical & Engineering Data,* vol. 41, pp. 1488-1494, 1996.

[131] J. Deschamps, D.-H. Menz, A. A. H. Padua, and M. F. C. Gomes, "Low pressure solubility and thermodynamics of solvation of oxygen, carbon dioxide, and carbon onoxide in fluorinated liqids," *Elsevier,* November 29 2006 2006.

[132] A. Weber, R. Pockelmann, and C.-P. Klages, "Electrical and optical properties of amorphous fluorocarbon films prepared by plasma polymerization of perfluoro-1,3-dimethylcyclohexane," *Journal of Vaccum Science & Technology A Vaccum Surfaces*

and Films, vol. 16, 1998.

[133] M.-J. Jeng, S.-S. Yang, M. R. Wolfson, and T. H. Shaffer, "Perfluorochemical (PFC) combinations for acute lung injury: an in vitro and in vivo study in juvenile rabbits," *Pediatric research,* vol. 53, pp. 81-88, 2003.

[134] M. F. Refojo, J. Friend, and F.-L. Leong, "Perfluoro-1-methyldecalin as a potential oxygen carrier with fluid scleral lenses," *Current eye research,* vol. 4, pp. 732-733, 1985.

[135] M. G. Freire, A. G. Ferreira, I. M. Fonseca, I. M. Marrucho, and J. A. Coutinho, "Viscosities of liquid fluorocompounds," *Journal of Chemical & Engineering Data,* vol. 53, pp. 538-542, 2008.

[136] A. Dias, A. Caço, J. Coutinho, L. Santos, M. Pineiro, L. Vega*, et al.*, "Thermodynamic properties of perfluoro-*n*-octane," *Fluid phase equilibria,* vol. 225, pp. 39-47, 2004.

[137] A. Kang and M. W. Chang, "Identification and reconstitution of genetic regulatory networks for improved microbial tolerance to isooctane," *Molecular BioSystems,* vol. 8, pp. 1350-1358, 2012.

[138] V. L. Tlapak-Simmons, C. A. Baron, and P. H. Weigel, "Characterization of the purified hyaluronan synthase from *Streptococcus equisimilis*," *Biochemistry,* vol. 43, pp. 9234-9242, 2004.

[139] T. H. Ngo and A. Schumpe, "Oxygen absorption into stirred emulsions of *n*-alkanes," *International Journal of Chemical Engineering,* vol. 2012, 2012.

[140] S. S. Alves and H. J. Pinho, "Gas Absorption in Stirred Gas-Liquid-Liquid Systems: Effect of Transferred Solute Solubility and Oil Phase Spreading Characteristics,"

Chemical Engineering Communications, vol. 200, pp. 1425-1442, 2013.

[141] A. Kundu, E. Dumont, A. M. Duquenne, and H. Delmas, "Mass transfer characteristics in gas‐liquid‐liquid system," *The canadian journal of chemical engineering,* vol. 81, pp. 640-646, 2003.

[142] M. Elibol and F. Mavituna, "A remedy to oxygen limitation problem in antibiotic production: addition of perfluorocarbon," *Biochemical engineering journal,* vol. 3, pp. 1-7, 1999.

[143] M. Elibol, "Mass transfer characteristics of yeast fermentation broth in the presence of pluronic F-68," *Process biochemistry,* vol. 34, pp. 557-561, 1999.

[144] P. H. Weigel, Z. Kyossev, and L. C. Torres, "Phospholipid dependence and liposome reconstitution of purified hyaluronan synthase," *Journal of Biological Chemistry,* vol. 281, pp. 36542-36551, December 1, 2006 2006.

[145] T. Hoffmann, B. Troup, A. Szabo, C. Hungerer, and D. Jahn, "The anaerobic life of *Bacillus subtilis*: cloning of the genes encoding the respiratory nitrate reductase system," *FEMS microbiology letters,* vol. 131, pp. 219-225, 1995.

[146] H. C. Ramos, L. Boursier, I. Moszer, F. Kunst, A. Danchin, and P. Glaser, "Anaerobic transcription activation in *Bacillus subtilis*: identification of distinct FNR-dependent and-independent regulatory mechanisms," *The EMBO journal,* vol. 14, p. 5984, 1995.

[147] P. H. Weigel, "Functional characteristics and catalytic mechanisms of the bacterial hyaluronan synthases," *IUBMB Life,* vol. 54, pp. 201-211, 2002.

[148] V. L. Tlapak-Simmons, E. S. Kempner, B. A. Baggenstoss, and P. H. Weigel, "The active streptococcal hyaluronan synthases (HASs) contain a single HAS monomer and

multiple cardiolipin molecules," *Journal of Biological Chemistry,* vol. 273, pp. 26100-26109, October 2, 1998 1998.

[149] P. H. Weigel and B. A. Baggenstoss, "Hyaluronan synthase polymerizing activity and control of product size are discrete enzyme functions that can be uncoupled by mutagenesis of conserved cysteines," *Glycobiology,* vol. 22, pp. 1302-1310, 2012.

[150] V. L. Tlapak-Simmons, B. A. Baggenstoss, T. Clyne, and P. H. Weigel, "Purification and lipid dependence of the recombinant hyaluronan synthases from *Streptococcus pyogenes* and *Streptococcus equisimilis*," *Journal of Biological Chemistry,* vol. 274, pp. 4239-4245, February 12, 1999 1999.

[151] T. Yoshimura, N. Shibata, Y. Hamano, and K. Yamanaka, "Heterologous production of hyaluronic acid in an ε-poly-L-lysine producer, *Streptomyces albulus*," *Applied and Environmental Microbiology,* vol. 81, pp. 3631-3640, June 1, 2015 2015.

[152] J. Sikkema, J. De Bont, and B. Poolman, "Mechanisms of membrane toxicity of hydrocarbons," *Microbiological reviews,* vol. 59, pp. 201-222, 1995.

[153] T. McIntosh, S. Simon, and R. MacDonald, "The organization of n-alkanes in lipid bilayers," *Biochimica et Biophysica Acta (BBA)-Biomembranes,* vol. 597, pp. 445-463, 1980.

[154] S. Paterson, K. Butler, P. Huang, J. Labelle, I. C. Smith, and H. Schneider, "The effects of alcohols on lipid bilayers: a spin label study," *Biochimica et Biophysica Acta (BBA)-Biomembranes,* vol. 266, pp. 597-602, 1972.

[155] C. Grisham and R. Barnett, "The effects of long-chain alcohols on membrane lipids and the (Na++ K+)-ATPase," *Biochimica et Biophysica Acta (BBA)-Biomembranes,* vol.

311, pp. 417-422, 1973.

[156] L. Ingram, "Adaptation of membrane lipids to alcohols," *Journal of Bacteriology,* vol. 125, pp. 670-678, 1976.

[157] L. Ingram, "Changes in lipid composition of *Escherichia coli* resulting from growth with organic solvents and with food additives," *Applied and environmental microbiology,* vol. 33, pp. 1233-1236, 1977.

[158] H.-J. Lehmler, "Anti-inflammatory effects of perfluorocarbon compounds," *Expert review of respiratory medicine,* vol. 2, pp. 273-289, 2008.

[159] R. Bronnenmeier and H. Märkl, "Hydrodynamic stress capacity of microorganisms," *Biotechnology and bioengineering,* vol. 24, pp. 553-578, 1982.

[160] M. Toma, M. Ruklisha, J. Vanags, M. Zeltina, M. Lelte, N. Galinine*, et al.*, "Inhibition of microbial growth and metabolism by excess turbulence," *Biotechnology and bioengineering,* vol. 38, pp. 552-556, 1991.

[161] S. Sahoo, R. K. Verma, A. Suresh, K. K. Rao, J. Bellare, and G. Suraishkumar, "Macro‐level and genetic‐level responses of *Bacillus subtilis* to shear stress," *Biotechnology progress,* vol. 19, pp. 1689-1696, 2003.

[162] T. Candela and A. Fouet, "Poly‐gamma‐glutamate in bacteria," *Molecular microbiology,* vol. 60, pp. 1091-1098, 2006.